Published OnlineFirst February 4, 2013; DOI: 10.1158/0008-5472.CAN-12-3479

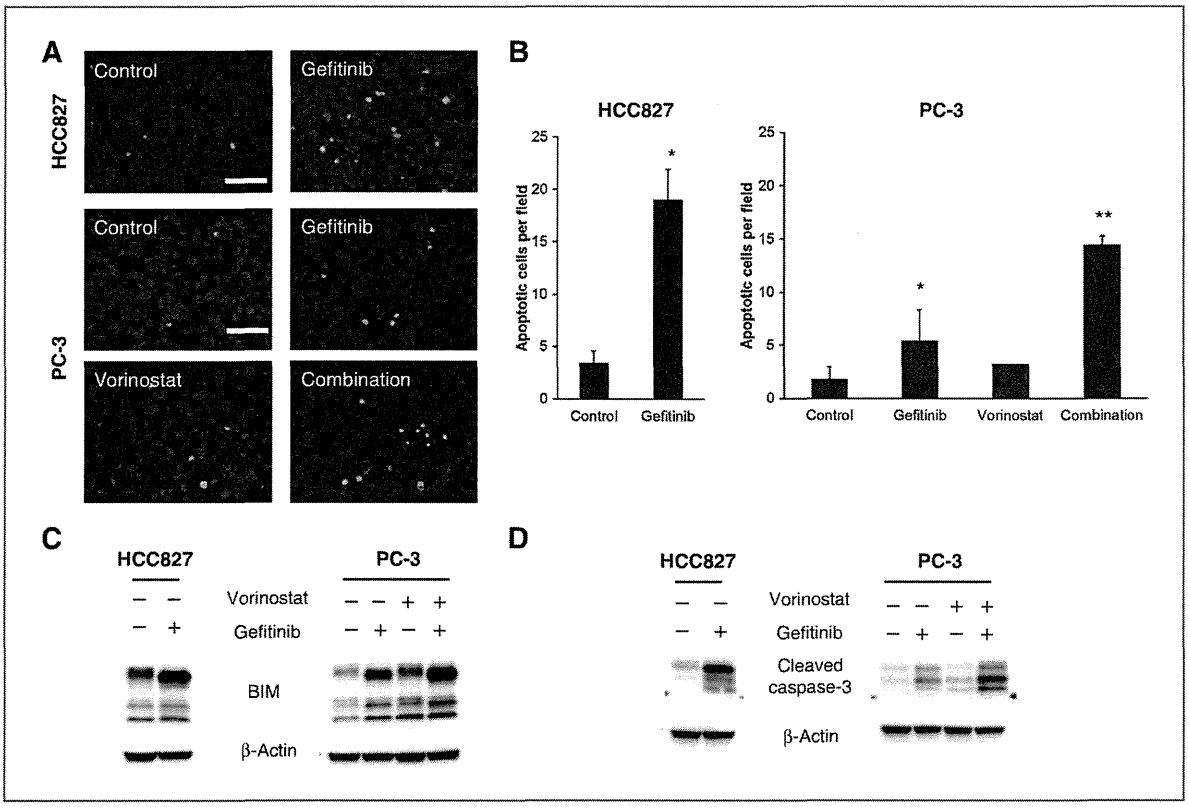

Figure 4. Vorinostat combined with gefitinib increases apoptosis in xenograft tumors with the *BIM* polymorphism. HCC827 and PC-3 xenograft tumors were resected from mice treated with 25 mg/kg gefitinib and/or 40mg/kg vorinostat for 4 days. A, analysis of apoptosis by TUNEL staining. Representative fluorescent images are shown. Green fluorescence indicates apoptotic cells. Bar indicates 50 μm. B, quantitation of number of apoptotic cells. *, $P < 0.05$ gefitinib or vorinostat versus control; **, $P < 0.05$ combination versus control and single agents. Bars represent mean ± SD. C, tumors were harvested 8 hours after 2 consecutive treatments with each compound, and the levels of protein in tumor lysates were determined by Western blotting. D, tumors were harvested 24 hours after 4 consecutive treatments with each compound. Protein expression levels in the tumor lysates were determined by Western blotting.

unselected patients with NSCLC, more than 65% of whom were Caucasian, failed to show therapeutic benefits (19). These findings suggest that the combination of vorinostat and an EGFR-TKI should be tested in selected patients with NSCLC with *EGFR* mutations and the *BIM* polymorphism.

Resistance to EGFR-TKIs associated with the *BIM* deletion polymorphism may be overcome by treatment with BH3 mimetics, such as ABT-737 (5). Although ABT-737 antagonized antiapoptotic proteins, such as Bcl-2 and Bcl-X_L, it did not antagonize the antiapoptotic protein Mcl-1, which is overexpressed in NSCLC (20), suggesting that the effects of BH3 mimetics may be limited to overcoming EGFR-TKI resistance caused by the *BIM* polymorphism in NSCLC. BH3 mimetics are being evaluated in early-phase clinical trials but are not ready for use in clinical practice. In contrast, vorinostat has been approved by the FDA for the treatment of patients with advanced primary cutaneous T-cell lymphoma (15). Therefore, the combination of gefitinib and vorinostat could easily be tested clinically.

The *BIM* polymorphism can be detected in formalin-fixed paraffin-embedded tumor tissues and peripheral blood (5). Moreover, a convenient and easy access PCR screening method can detect this polymorphism in circulating DNA from serum (Supplementary Fig. S5A and S5B). As the *BIM* polymorphism is a germline alteration, it can be assayed in serum obtained at any time point. Collectively, our findings illustrate the importance of clinical trials testing the ability of combinations of vorinostat and EGFR-TKIs to overcome EGFR-TKI resistance associated with the *BIM* polymorphism in patients with *EGFR*--mutant NSCLC.

Disclosure of Potential Conflicts of Interest

T. Nakagawa is an employee of Eisai Co., Ltd. for oncology research. Y. Hasegawa received research funding from Chugai Pharmaceutical Co., Ltd., Merck Sharp & Dohme Corp., AstraZeneca, and TAIHO Pharmaceutical Co., Ltd. S. Yano received honoraria from Chugai Pharmaceutical Co., Ltd. and AstraZeneca and received research funding from Chugai Pharmaceutical Co., Ltd., Kyowa Hakko Kirin Co., Ltd., and Eisai Co., Ltd. No potential conflicts of interest were disclosed by the other authors.

Authors' Contributions

Conception and design: T. Nakagawa, S. Takeuchi, S. Nanjo, S. Yano
Development of methodology: T. Nakagawa, S. Takeuchi
Acquisition of data (provided animals, acquired and managed patients, provided facilities, etc.): T. Nakagawa, D. Ishikawa, Y. Hasegawa

Published OnlineFirst February 4, 2013; DOI: 10.1158/0008-5472.CAN-12-3479

Analysis and interpretation of data (e.g., statistical analysis, biostatistics, computational analysis): T. Nakagawa, S. Yano
Writing, review, and/or revision of the manuscript: T. Nakagawa, S. Takeuchi, H. Ebi, M. Sato, Y. Hasegawa, Y. Sekido, S. Yano
Administrative, technical, or material support (i.e., reporting or organizing data, constructing databases): T. Yamada, T. Sano, M. Sato, Y. Sekido
Study supervision: S. Takeuchi, Y. Sekido, S. Yano

Acknowledgments

The authors thank Dr. John Minna (University of Texas Southwestern Medical Center) for the HCC2279 cells.

Grant Support

This study was supported by Grants-in-Aid for Cancer Research (21390256 to S. Yano; 11019957 to S. Takeuchi), Scientific Research on Innovative Areas "Integrative Research on Cancer Microenvironment Network" (22112010A01 to S. Yano), and Grant-in-Aid for Project for Development of Innovative Research on Cancer Therapeutics (P-Direct) from the Ministry of Education, Culture, Sports, Science, and Technology (MEXT) of Japan.

Received September 3, 2012; revised December 20, 2012; accepted January 19, 2013; published OnlineFirst February 4, 2013.

References

1. Maemondo M, Inoue A, Kobayashi K, Sugawara S, Oizumi S, Isobe H, et al.North-East Japan Study Group. Gefitinib or chemotherapy for non-small-cell lung cancer with mutated EGFR. N Engl J Med 2010;362:2380–8.
2. Pao W, Chmielecki J. Rational, biologically based treatment of EGFR-mutant non-small-cell lung cancer. Nat Rev Cancer 2010;10:760–74.
3. Sequist LV, Waltman BA, Dias-Santagata D, Digumarthy S, Turke AB, Fidias P, et al. Genotypic and histological evolution of lung cancers acquiring resistance to EGFR inhibitors. Sci Transl Med 2011; 3:75ra26.
4. Yano S, Wang W, Li Q, Matsumoto K, Sakurama H, Nakamura T, et al. Hepatocyte growth factor induces gefitinib resistance of lung adenocarcinoma with epidermal growth factor receptor-activating mutations. Cancer Res 2008;68:9479–87.
5. Ng KP, Hillmer AM, Chuah CT, Juan WC, Ko TK, Teo AS, et al. A common BIM deletion polymorphism mediates intrinsic resistance and inferior responses to tyrosine kinase inhibitors in cancer. Nat Med 2012;18:521–8.
6. O'Connor L, Strasser A, O'Reilly LA, Hausmann G, Adams JM, Cory S, et al. Bim: a novel member of the Bcl-2 family that promotes apoptosis. EMBO J 1998;17:384–95.
7. Chen L, Willis SN, Wei A, Smith BJ, Fletcher JI, Hinds MG, et al. Differential targeting of prosurvival Bcl-2 proteins by their BH3-only ligands allows complementary apoptotic function. Mol Cell 2005;17: 393–403.
8. Heath-Engel HM, Shore GC. Regulated targeting of Bax and Bak to intracellular membranes during apoptosis. Cell Death Differ 2006;13: 1277–80.
9. Costa DB, Halmos B, Kumar A, Schumer ST, Huberman MS, Boggon TJ, et al. BIM mediates EGFR tyrosine kinase inhibitor-induced apoptosis in lung cancers with oncogenic EGFR mutations. PLoS Med 2007;4:1669–79.
10. Fukazawa H, Noguchi K, Masumi A, Murakami Y, Uehara Y. BimEL is an important determinant for induction of anoikis sensitivity by mitogen-activated protein/extracellular signal-regulated kinase kinase inhibitors. Mol Cancer Ther 2004;3:1281–8.
11. Liu JW, Chandra D, Tang SH, Chopra D, Tang DG. Identification and characterization of Bimgamma, a novel proapoptotic BH3-only splice variant of Bim. Cancer Res 2002;62:2976–81.
12. Faber AC, Corcoran RB, Ebi H, Sequist LV, Waltman BA, Chung E, et al. BIM expression in treatment-naive cancers predicts responsiveness to kinase inhibitors. Cancer Discov 2011;1:352–65.
13. Bolden JE, Peart MJ, Johnstone RW. Anticancer activities of histone deacetylase inhibitors. Nat Rev Drug Discov 2006;5:769–84.
14. Mann BS, Johnson JR, Cohen MH, Justice R, Pazdur R. FDA approval summary: vorinostat for treatment of advanced primary cutaneous T-cell lymphoma. Oncologist 2007;12:1247–52.
15. Xargay-Torrent S, Lopez-Guerra M, Saborit-Villarroya I, Rosich L, Campo E, Roue G, et al. Vorinostat-induced apoptosis in mantle cell lymphoma is mediated by acetylation of proapoptotic BH3-only gene promoters. Clin Cancer Res 2011;17:3956–68.
16. Delcuve GP, Khan DH, Davie JR. Roles of histone deacetylases in epigenetic regulation: emerging paradigms from studies with inhibitors. Clin Epigenetics 2012;4:5.
17. Sharma SV, Lee DY, Li B, Quinlan MP, Takahashi F, Maheswaran S, et al. A chromatin-mediated reversible drug-tolerant state in cancer cell subpopulations. Cell 2010;141:69–80.
18. Witta SE, Gemmill RM, Hirsch FR, Coldren CD, Hedman K, Ravdel L, et al. Restoring E-cadherin expression increases sensitivity to epidermal growth factor receptor inhibitors in lung cancer cell lines. Cancer Res 2006;66:944–50.
19. Witta SE, Jotte RM, Konduri K, Neubauer MA, Spira AI, Ruxer RL, et al. Randomized phase II trial of erlotinib with and without entinostat in patients with advanced non-small-cell lung cancer who progressed on prior chemotherapy. J Clin Oncol 2012;30:2248–55.
20. Cetin Z, Ozbilim G, Erdogan A, Luleci G, Karauzum SB. Evaluation of PTEN and Mcl-1 expressions in NSCLC expressing wild-type or mutated EGFR. Med Oncol 2010;27:853–60.

The American Journal of Pathology, Vol. 182, No. 5, May 2013

ELSEVIER

The American Journal of
PATHOLOGY

ajp.amjpathol.org

TUMORIGENESIS AND NEOPLASTIC PROGRESSION

Surfactant Protein A Suppresses Lung Cancer Progression by Regulating the Polarization of Tumor-Associated Macrophages

Atsushi Mitsuhashi,* Hisatsugu Goto,* Takuya Kuramoto,* Sho Tabata,* Sawaka Yukishige,* Shinji Abe,* Masaki Hanibuchi,* Soji Kakiuchi,* Atsuro Saijo,* Yoshinori Aono,* Hisanori Uehara,† Seiji Yano,‡ Julie G. Ledford,§ Saburo Sone,* and Yasuhiko Nishioka*

From the Departments of Respiratory Medicine and Rheumatology and Molecular and Environmental Pathology,† Institute of Health Biosciences, The University of Tokushima Graduate School, Tokushima, Japan; the Division of Medical Oncology,‡ Cancer Research Institute, Kanazawa University, Kanazawa, Japan; and the Division of Pulmonary, Allergy, and Critical Care Medicine,§ Duke University Medical Center, Durham, North Carolina*

Accepted for publication January 10, 2013.

Address correspondence to Yasuhiko Nishioka, M.D., Ph.D., Department of Respiratory Medicine and Rheumatology, Institute of Health Biosciences, The University of Tokushima Graduate School. 3-18-15 Kuramoto-cho Tokushima, 770-8503, Japan. E-mail: yasuhiko@clin.med.tokushima-u.ac.jp.

Surfactant protein A (SP-A) is a large multimeric protein found in the lungs. In addition to its immunoregulatory function in infectious respiratory diseases, SP-A is also used as a marker of lung adenocarcinoma. Despite the finding that SP-A expression levels in cancer cells has a relationship with patient prognosis, the function of SP-A in lung cancer progression is unknown. We investigated the role of SP-A in lung cancer progression by introducing the SP-A gene into human lung adenocarcinoma cell lines. SP-A gene transduction suppressed the progression of tumor in subcutaneous xenograft or lung metastasis mouse models. Immunohistochemical analysis showed that the number of M1 antitumor tumor-associated macrophages (TAMs) was increased and the number of M2 tumor-promoting TAMs was not changed in the tumor tissue produced by SP-A–expressing cells. In addition, natural killer (NK) cells were also increased and activated in the SP-A–expressing tumor. Moreover, SP-A did not inhibit tumor progression in mice depleted of NK cells. Taking into account that SP-A did not directly activate NK cells, these results suggest that SP-A inhibited lung cancer progression by recruiting and activating NK cells via controlling the polarization of TAMs. *(Am J Pathol 2013, 182: 1843–1853; http://dx.doi.org/10.1016/j.ajpath.2013.01.030)*

Lung cancer is the major cause of malignancy-related death worldwide. Mortality is 80% to 90%, which makes this disease the leading cause of cancer-related deaths.[1] The high mortality rate of this disease is primarily due to the difficulty of early diagnosis, the high metastatic potential, and the poor responses to chemical therapy and radiotherapy. Because there is no established curative therapy for advanced lung cancer to date, clinical management is palliative in many cases. Therefore, it is crucial to investigate and understand the underlying biological and molecular mechanisms of lung cancer progression.

Surfactant protein A (SP-A) is a large multimeric protein found in the airways and alveoli of the lungs. SP-A is a member of the collectin family of proteins, characterized by NH_2-terminal collagen-like regions and COOH-terminal lectin domains. Although other SPs, such as SP-B, function to reduce surface tension in the lungs, SP-A (and SP-D) regulates the pulmonary immune response.[2] Previous *in vivo* studies have shown that SP-A regulates responses involved in initiation and potentiation of inflammation by regulating the production of proinflammatory cytokines, such as tumor necrosis factor α (TNF-α), in response to lipopolysaccharide[3] or by accelerating the clearance of a variety of pathogens.[4–8] Because SP-A has the ability to opsonize and enhance pathogen uptake by phagocytes, the immunoregulatory roles of SP-A have been studied mainly in the field of infectious diseases. Recently, we reported that

Supported by the Ministry of Education, Culture, Sports, Science and Technology Grants-in Aid for Scientific Research (MEXT KAKENHI) grant 22790759 (H.G.) and NIH grants AI-81672 and HL-111151 (J.G.L.).

A.M. and H.G. contributed equally to this work.

http://dx.doi.org/10.1016/j.ajpath.2013.01.030

SP-A has a role in regulating bleomycin-induced acute noninfectious lung injury by inhibiting lung epithelial cell apoptosis.[9] Pastva et al[10] reported that SP-A regulates T_H2 cytokine production in a mouse asthma model. These results suggest that SP-A has diverse functions to control various lung diseases. Considering that SP-A contributes to multiple aspects of pulmonary host defense, we hypothesized that SP-A might have a role in lung cancer progression.

In a lung cancer study, SP-A was expressed in approximately 49% of primary non–small cell lung carcinomas[11] and is used as a specific marker of carcinoma that originates in type II pneumocytes. In addition, a previous study demonstrated that deletion of the *SFTPA1* (alias, *SPA*) gene in non–small cell lung cancer cells was associated with tumor progression.[12] Tsutsumida et al[13] found that patients with lung adenocarcinoma with relatively high MUC1 mucin expression and low SP-A expression in cancer cells had a poor outcome. These clinical studies demonstrate that in addition to use as a diagnostic marker, SP-A expression in lung cancer cells could be a useful biomarker of good prognosis. Although these studies suggested that SP-A might have a role in suppressing lung cancer progression, the role of SP-A in lung cancer has not been extensively studied, and the mechanisms by which SP-A controls lung cancer progression remain unknown.

In this study, we generated SP-A–overexpressing human lung adenocarcinoma cells and evaluated the role of SP-A in lung cancer progression using experimental mouse models.

Materials and Methods

Cell Lines

The human lung adenocarcinoma cell line PC14PE6 was a gift from Dr. Isaiah J. Fidler (The University of Texas MD Anderson Cancer Center, Houston TX). The human lung adenocarcinoma cell line A549 was purchased from ATCC (Manassas, VA). These cell lines were authenticated by BEX Co. Ltd. (Tokyo, Japan) using a multiplex short tandem repeat assay. Both cell lines were maintained in RPMI 1640 medium supplemented with 10% heat-inactivated fetal bovine serum, 100 U/mL of penicillin, and 50 μg/mL of streptomycin and were cultured at 37°C in a humidified atmosphere of 5% CO_2 in air.

Reagents

An anti-mouse IL-2 receptor β-chain monoclonal antibody, TM-β1 (IgG2b), was a gift from Drs. Masayuki Miyasaka and Toshio Tanaka (Osaka University, Osaka, Japan).

SP-A Purification

SP-A was purified from the lung lavage fluid of patients with alveolar proteinosis as previously described[14] and was routinely tested to reduce endotoxin contamination.[14] Briefly, SP-A was suspended in 100 mmol/L octylglucoside and 5 mmol/L Tris, pH 7.4, after butanol extraction.

Table 1 Primer Sequences Used in Quantitative PCR

	Forward	Reverse	Product size (bp)
Gene (mouse)			
IL-1β	5′-TGACGTTCCCATTAGACAAC-3′	5′-ATTTTGTCGTTGCTTGGTTC-3′	171
IL-6	5′-GTACCATAGCTACCTGGAGT-3′	5′-GGAAATTGGGGTAGGAAGGA-3, ′	154
TNF-α	5′-CCTATGTCTCAGCCTCTTCT-3′	5′-TTGGGAACTTCTCATCCCTT-3′	107
IL-12	5′-CACACTGGACCAAAGGGACT-3′	5′-TGGTTTGATGATGTCCCTGA-3′	169
IFN-γ	5′-TAGCTCTGAGACAATGAACG-3′	5′-CACATCTATGCCACTTGAGT-3′	145
CCL2	5′-TTCACAGTTGCCGGCTGG-3′	5′-TGAATGAGTAGCAGCAGGTGAGTG-3′	81
CCL5	5′-CAGCAGCAAGTGCTCCAATCTT-3′	5′-TTCTTGAACCCACTTCTTCTCTGG-3′	91
IL-10	5′-AAGGACCAGCTGGACAACAT-3′	5′-TCTCACCCAGGGAATTCAAA-3′	172
MRC-1	5′-TGCAAGGATCATACTTCCCT-3′	5′-TGATGTTCTCCAGTAGCCAT-3′	240
Arg1	5′-GAATGGAAGAGTCAGTGTGG-3′	5′-AATGACACATAGGTCAGGGT-3′	97
CD163	5′-GACGACAGATTCAGCGACTT-3′	5′-CCGAGGATTTCAGCAAGTCCA-3′	114
Prf1	5′-GACACAGTAGAGTGTCGCAT-3′	5′-TTTTGAAGTCAAGGTGGAGTG-3′	70
GzmB	5′-AGAGAGCAAGGACAACACTC-3′	5′-ATCGAAAGTAAGGCCATGTAG-3′	176
B2M (β_2M)	5′-GGAAGCCGAACATACTGAACTG-3′	5′-TTTCCCGTTCTTCAGCATTTGG-3′	80
Gene (human)			
IL-1β	5′-GACAGGATATGGAGCAACAA-3′	5′-GCTGTAGAGTGGGCTTATCA-3′	147
IL-6	5′-CCTCTTCAGAACGAATTGAC-3′	5′-AGTCTCCTCATTGAATCCAG-3′	186
TNF-α	5′-GGCAGTCAGATCATCTTCTCG-3′	5′-CAGCTGGTTATCTCTCAGCTC-3′	148
CCL2	5′-CTCATAGCAGCCACCTTCATT-3′	5′-ACAGATCTCCTTGGCCACAA-3′	192
CCL3	5′-GGCAGTCAGATCATCTTCTCG-3′	5′-CAGCTGGTTATCTCTCAGCTC-3 ′	81
CCL5	5′-CTGTCATCCTCATTGCTACTG-3′	5′-GCCACTGGTGTAGAAATACTC-3′	140
MRC-1	5′-CCATCGAGGAATTGGACTTT-3′	5′-TGTCATTTAAGCCGATCCAC-3′	78
RPL27	5′-ATCGCCAAGAGATCAAAGATAA-3′	5′-TCTGAAGACATCCTTATTGACG-3′	123

Polymyxin-agarose (Sigma-Aldrich, St. Louis, MO) was added 1:5 (v/v) and allowed to incubate at room temperature for 30 minutes. The mixture was then dialyzed (14,000 molecular weight cutoff value) for four changes ≥4 hours each against autoclaved 5 mmol/L Tris, pH 7.4. The mixture was then centrifuged, and the supernatant, containing SP-A, was removed by gentle aspiration. SP-A preparations had final endotoxin concentrations of <0.1 pg/μg of SP-A as determined by the Limulus amoebocyte lysate assay (QCL-1000; BioWhittaker, Walkersville, MD).

SPA Gene Transduction

The human *SPA* gene–expressed region [SFTPA1 (NM_005411)] (OriGene Technologies, Rockville, MD) was introduced into the pMIG vector (a gift from Dr. Alana L. Welm, University of Utah, Salt Lake City). The Platinum-E packaging cell line (a gift from Dr. Toshio Kitamura, Tokyo University, Tokyo, Japan)[15] was transfected with pMIG or derivative vector DNA by using FuGENE 6 transfection reagent (Roche Applied Science, Indianapolis, IN). PC14PE6 or A549 cells were infected using the viral supernatant as described previously.[16] The proportion of green fluorescent protein–positive cells was >90% in the entire population.

Animals

Male athymic BALB/c nude mice and SCID mice were obtained from Charles River Laboratories Japan (Yokohama) and CLEA Japan (Tokyo), respectively, and were maintained under specific pathogen-free conditions throughout the study. All the experiments were performed in accordance with the guidelines established by The University of Tokushima Committee on Animal Care and Use, Tokushima, Japan. At the end of each *in vivo* experiment, the mice were anesthetized with isoflurane and euthanized humanely by cutting the subclavian artery. All the experiment protocols were reviewed and approved by the Animal Research Committee of The University of Tokushima.

In Vivo Subcutaneous Xenograft Model

PC14PE6 cells (1.0×10^6 per mouse) or A549 cells (3.0×10^6 per mouse) suspended in 0.1 mL of PBS were subcutaneously inoculated into the right flank of nude mice. Tumor size was measured using a vernier caliper three times a week (volume = $ab^2/2$, where a indicates long diameter; b, short diameter). The mice were euthanized humanely on day 21, and the tumors were resected for further analyses.

In Vivo Lung Metastasis Model

To establish lung metastasis, nude mice were intravenously inoculated via the tail vein with 1.0×10^6 tumor cells per mouse.[17] The mice were euthanized humanely on either day 28 (PC14PE6) or day 42 (A549). The lungs were weighed, and the number of metastatic colonies on the surface of the lungs was determined by visual examination. Because PC14PE6 cells produce large amounts of pleural effusion,[18] the volume of the effusion was also evaluated. In some experiments, natural killer (NK) cells were depleted by treating nude mice with TM-β1 5 days after inoculation of PC14PE6 cells.[19]

Immunofluorescence

The excised tumor tissue was placed into OCT compound (Sakura Finetechnical Co., Tokyo, Japan) and snap frozen. Eight-micrometer-thick frozen tissue sections were fixed with 4% paraformaldehyde solution in PBS and were used for identification of macrophages using 1:150 rat anti-mouse CD68 monoclonal antibody (Serotec, Oxford, UK) and of NK cells using 1:100 goat anti-mouse NKp46/NCR1 monoclonal antibody (R&D Systems, Minneapolis, MN). Alexa Fluor 488–labeled secondary antibodies (dilution 1:250; Invitrogen, Carlsbad, CA) were used for immunofluorescence (IF) detection. To identify M1 or M2 macrophages, the sections were stained with 1:150 fluorescein isothiocyanate–conjugated rat anti-mouse TNF-α antibody (BD Pharmingen, Franklin Lakes, NJ) or 1:150 fluorescein isothiocyanate–conjugated rat anti-mouse CD206 [mannose

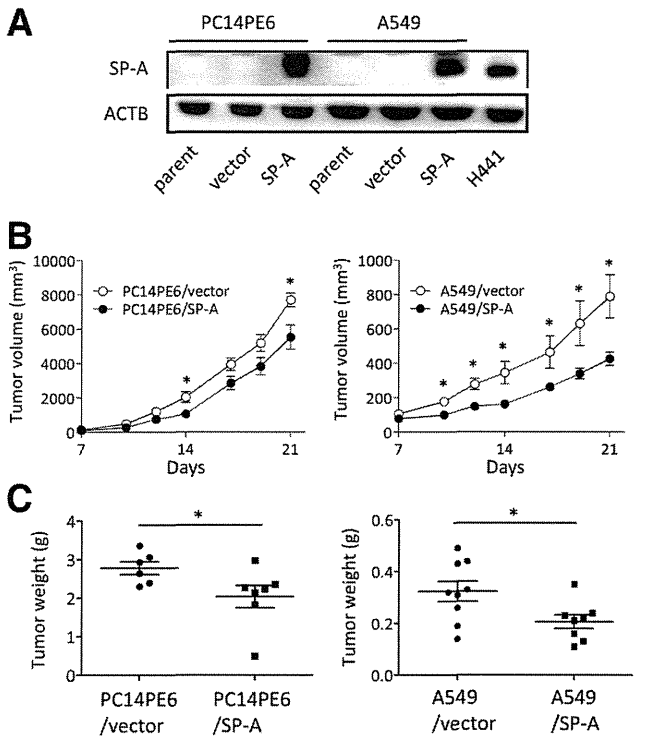

Figure 1 The effect of SP-A on lung cancer subcutaneous xenografts *in vivo*. **A:** SP-A expression of human SP-A stable transfectants was confirmed by Western blot analysis. H441 cells were used as a positive control. ACTB, β-actin. Tumor growth (**B**) and weight (**C**) of xenografts produced by PC14PE6 (**left panels**; $n = 6$ per group) and A549 (**right panels**; $n = 8$ per group) cells transduced with SP-A or vector. Data are presented as means ± SEM (**horizontal lines** in **C**). $^*P < 0.05$.

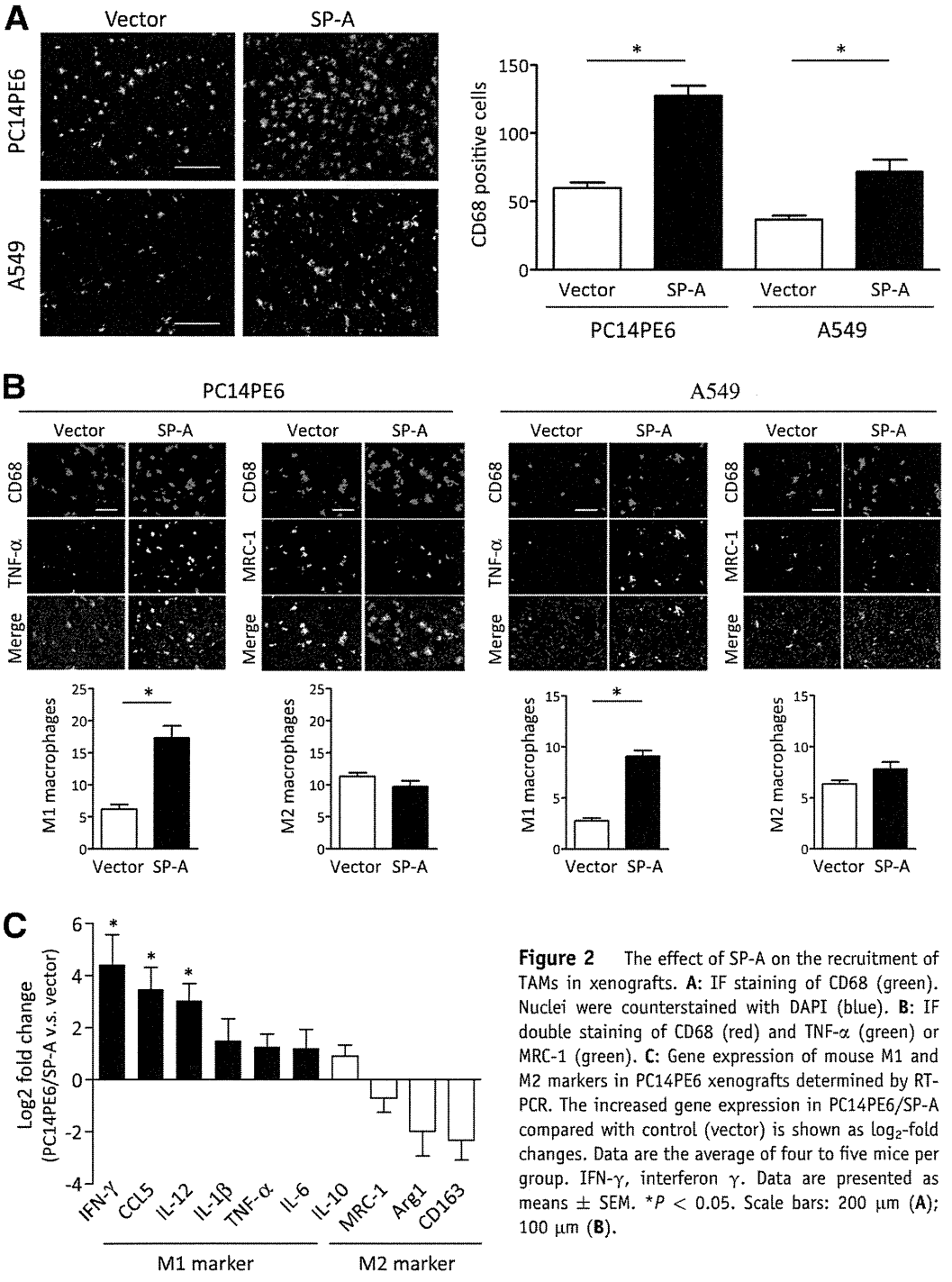

Figure 2 The effect of SP-A on the recruitment of TAMs in xenografts. **A**: IF staining of CD68 (green). Nuclei were counterstained with DAPI (blue). **B**: IF double staining of CD68 (red) and TNF-α (green) or MRC-1 (green). **C**: Gene expression of mouse M1 and M2 markers in PC14PE6 xenografts determined by RT-PCR. The increased gene expression in PC14PE6/SP-A compared with control (vector) is shown as $\log_2$-fold changes. Data are the average of four to five mice per group. IFN-γ, interferon γ. Data are presented as means ± SEM. $^*P < 0.05$. Scale bars: 200 μm (**A**); 100 μm (**B**).

receptor C type 1 (MRC-1)] antibody (BioLegend, San Diego, CA) after CD68 staining. Alexa Fluor 594–labeled anti-rat secondary antibodies (dilution 1:250; Invitrogen) were used for CD68 IF detection. M1 or M2 macrophages were identified as CD68-positive/TNF-α-–positive or CD68-positive/MRC-1–positive cells, respectively. Nuclei were counterstained with DAPI (blue). In each slide, the number of positive cells was counted in five areas under fluorescent microscopy at ×100 (single staining) or ×200 (double staining) magnification.

RT-qPCR

Total RNA was extracted from the tumors using the RNeasy mini kit (Qiagen, Valencia, CA) and reverse transcribed to cDNA using a high-capacity cDNA Reverse Transcription kit (Applied Biosystems, Carlsbad, CA) according to the manufacturer's instructions. RT-PCR was performed using the CFX96 real-time PCR system (Bio-Rad Laboratories, Hercules, CA) using SYBR Premix Ex Taq (Takara, Kyoto, Japan). Human RPL27[20] and mouse β2m mRNA were used

as housekeeping genes, and quantification was determined by using the $\Delta\Delta C_T$ method. Specific PCR primer pairs for each studied gene are shown in Table 1.

SP-A Stimulation of Monocytes, Macrophages, and NK Cells

Human monocytes were separated from the peripheral blood of healthy volunteers as described previously.[21] The purity and viability of the monocytes was confirmed to be >98% by staining with Diff-Quik (Baxter Diagnostics, Deerfield, IL) and trypan blue, respectively. Mouse alveolar macrophages (AMs) were collected by using bronchoalveolar lavage as described previously.[9] More than 95% of the cells were confirmed to be AMs. For eliciting mouse peritoneal macrophages (PMs), 2 mL of thioglycollate (BD Biosciences, San Jose, CA) was injected into the peritoneal cavity of SCID mice. After 3 days, peritoneal exudative cells were harvested by intraperitoneal lavage with ice-cold PBS. Approximately 80% of isolated cells were macrophages. NK cells from SCID mice were isolated as previously described.[22] These immune cells were stimulated with 20 μg/mL of human SP-A for 4 hours in RPMI 1640 medium containing 1% fetal bovine serum. Total RNA was extracted for quantitative RT-PCR.

Cell Migration Assay

The migration assay was performed using 8-μm pore size cell culture inserts (BD Biosciences). After 24 hours of serum starvation, PMs in serum-free media were added to the inner chamber in the presence or absence of 20 μg/mL of SP-A. RPMI 1640 medium containing 10% fetal bovine serum was added to the lower chamber. After 17 hours of incubation, the cells that had migrated to the bottom surface of the filter were counted in six randomly selected fields on each filter under a microscope at ×200 magnification.

Western Blot Analysis

Twenty micrograms of total protein extracted from tumor cell lines was resolved by SDS-PAGE (Invitrogen) and was transferred to polyvinylidene difluoride membrane (Atto Corp., Tokyo, Japan), and Western blot was performed as described previously.[9] Immunoreactive bands were visualized using SuperSignal west femto maximum sensitivity substrate (Thermo Scientific, Waltham, MA).

Statistical Analysis

Data are given as means ± SEM. Statistical analysis was performed using the Student's *t*-test of unpaired samples or the *U*-test. Values of $P < 0.05$ were considered statistically significant.

Results

Effect of SP-A on Lung Cancer Xenografts *in Vivo*

Human lung adenocarcinoma cell lines (PC14PE6 and A549 cells) were transduced with vectors encoding human SP-A by the retroviral transduction system (termed PC14PE6/SP-A and A549/SP-A, respectively). The empty vector was transduced as a control (termed PC14PE6/vector and A549/vector, respectively) (Figure 1A). To investigate the effect of SP-A on *in vivo* tumor growth, we initially injected male nude mice subcutaneously with these cells. For both cell lines, the growth of xenografts was significantly inhibited when cells were overexpressing SP-A compared with the vector control cells (Figure 1, B and C).

Direct Effect of SP-A on Lung Cancer Cell Proliferation

To explore the underlying mechanism by which SP-A suppressed the growth of xenografts, we performed immunohistochemical staining of Ki-67, CD31, or TUNEL (Supplemental Figure S1A). The number of Ki-67–positive cells was significantly decreased in tumors formed by SP-A overexpressing PC14PE6 cells, whereas no difference was seen in A549 cells. The number of TUNEL-positive cells was increased in both cell lines expressing SP-A. No difference was seen in the number of CD31-positive cells. These results led us to consider that SP-A might have a direct effect on cancer cell proliferation or the cell

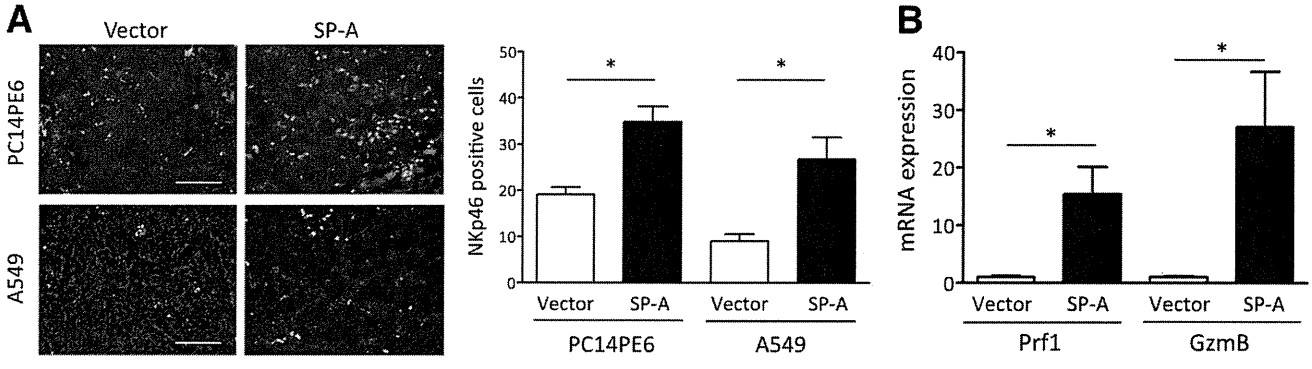

Figure 3 The effect of SP-A on NK cell recruitment in xenografts. **A:** IF staining of NKp46 (green). Nuclei were counterstained with DAPI (blue). Scale bars: 200 μm. **B:** Gene expression of mouse Prf1 and GzmB in PC14PE6 xenografts determined by RT-PCR. Data are the average of four to five mice per group. Data are presented as means ± SEM. *$P < 0.05$.

cycle. However, results of the *in vitro* MTT assay showed that SP-A–overexpressing cells had the same ability of cell proliferation with control cells in PC14PE6 and A549 cells (Supplemental Figure S1B). Propidium iodide staining revealed that the state of cell cycle and death was also similar by SP-A transduction in PC14PE6 cells (Supplemental Figure S1C). Moreover, the effect of SP-A on the cell cycle in PC14PE6 cells was also investigated by using the fluorescent ubiquitination-based cell-cycle indicator system, but no difference was observed (data not shown). Taken together, we considered that although SP-A inhibited tumor growth *in vivo*, its effect was not due to the direct effect on cell proliferation or the cell cycle or to the inhibition of tumor angiogenesis.

Effect of SP-A on the Recruitment of Tumor-Associated Macrophages

We next investigated whether cancer cell–produced SP-A might affect the tumor microenvironment. A variety of studies have shown that tumor-infiltrated tumor-associated macrophages (TAMs) play an important role in the progression of various types of cancers, including lung cancer.[23,24] It is also known that activated macrophages are functionally polarized into either M1 (classically activated) or M2 (alternatively activated) macrophages. M1 macrophages produce large amounts of inflammatory cytokines, such as TNF-α and interferon-γ, and are essential for tumor suppression and host defense against bacteria.[25] In contrast, M2 macrophages play important roles in tumor progression, tissue remodeling, and angiogenesis. M2 macrophages are characterized by their high expression of several factors, such as arginase-1, MRC-1, and IL-10. To determine whether SP-A affects the recruitment of TAMs, sections from resected tumors were subjected to IF staining. As shown in Figure 2A, the number of CD68-positive macrophages was significantly increased in tumors formed by SP-A–transduced cells. We then assessed whether M1 and M2 macrophage polarizations were altered by SP-A transduction. We performed IF double staining of CD68 and TNF-α for M1 and MRC-1 for M2 and determined M1 and M2 macrophages in the xenografts. In both SP-A–transduced cell lines, the number of M1 macrophages was significantly increased versus vector controls, whereas the number of M2 macrophages was not changed (Figure 2B). To confirm that the number of M1 macrophages was increased in the SP-A–expressing tumors, mRNA was extracted from the resected tumor, and the expression of M1 and M2 markers was determined by RT-PCR using mouse-specific primers. Multiple M1 markers were up-regulated in the SP-A–expressing tumors, whereas M2 markers were not changed compared with the vector control tumors (Figure 2C).

Effect of SP-A on NK Cell Recruitment in Xenografts

We next focused on the other important immune cells, NK cells. Because cytokines/chemokines such as interferon-γ, CCL5, and IL-12 that were up-regulated in the SP-A–expressing tumors are known to be potent inducers of NK cells,[26,27] we hypothesized that the *in vivo* tumor regression could be due to the recruitment of NK cells. Thus, we performed IF staining of NKp46 to determine the number of NK cells in the xenografts. As shown in Figure 3A, the number of

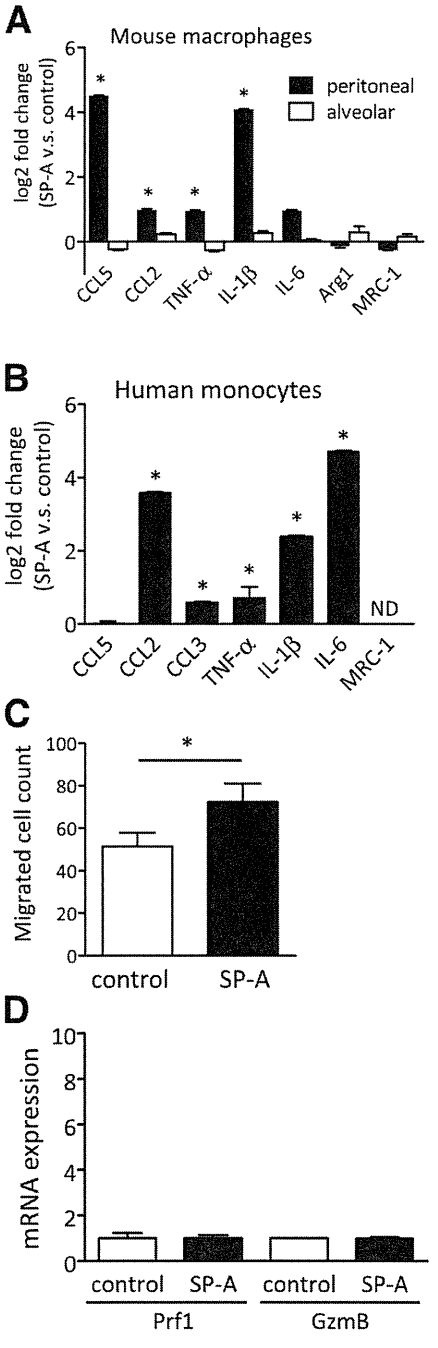

Figure 4 The effect of SP-A on various immune cells *in vitro*. After exogenous SP-A treatment, the expression of various genes was determined by RT-PCR in mouse PMs and AMs (**A**) and human peripheral monocytes (**B**). The increased gene expression in SP-A treatment compared with control (PBS) are shown as $\log_2$-fold changes ($n = 3$ per group). ND, not detected. **C**: The effect of exogenous SP-A on the migration of mouse PMs ($n = 3$ per group). **D**: Gene expressions of Prf1 and GzmB in mouse NK cells treated with exogenous SP-A ($n = 3$ per group). Data are presented as means ± SEM. $^*P < 0.05$.

Table 2 Effect of SP-A on Lung Metastasis Produced by Lung Adenocarcinoma Cell Lines in Nude Mice

	Lung			Pleural effusion	
		Metastasis			
Cell line	Weight (g)	Incidence	No.	Incidence	Volume (μL)
PC14PE6					
Vector	0.36 (0.30–0.42)	6/6	117.7 (67–183)	5/6	176.7 (0–300)
SP-A	0.27 (0.22–0.31)*	6/6	58.8 (21–111)*	0/6	All 0*
A549					
Vector	0.48 (0.30–0.85)	9/9	All >200		
SP-A	0.26 (0.19–0.41)†	10/10	All >200		

PC14PE6 or A549 cells (1×10^6 per mouse) were i.v. injected into nude mice, and lung metastasis and pleural effusion were evaluated. Values are means (ranges).

*Statistically significant difference compared with PC14PE6/vector ($P < 0.05$).

†Statistically significant difference compared with A549/vector ($P < 0.05$).

recruited NK cells was significantly increased in the SP-A–expressing tumors. Moreover, the expression of mouse perforin 1 (Prf1) and granzyme B (GzmB), key factors produced by NK cells to exhibit cell killing, was strongly up-regulated in SP-A–expressing tumors (Figure 3B), suggesting that NK cell killing was activated by SP-A in the tumor microenvironment. Collectively, these results indicate that in the tumor microenvironment, SP-A led to increased numbers of activated M1 TAMs and NK cells, which, in turn, can inhibit tumor growth.

Effect of SP-A on Macrophages and NK Cells *in Vitro*

Given the observation that the numbers of M1 macrophages and NK cells were increased in SP-A–expressing tumors, we performed *in vitro* experiments using thioglycollate-elicted mouse PMs, AMs, NK cells, and human peripheral blood monocytes to further examine the effect of SP-A on these cells. As shown in Figure 4A, exogenous SP-A treatment increased the expression of M1-related genes, such as CCL5, CCL2, TNF-α, and IL-1β, in mouse PMs. The expression of M2 markers did not change significantly. M1-related gene expression on human peripheral blood monocytes was also up-regulated by SP-A (Figure 4B). These results indicate that monocytes and macrophages can be directly targeted and activated toward the M1 phenotype by SP-A. Furthermore, the migration activity of PMs was increased by SP-A treatment (Figure 4C). Mouse AMs were not affected by exogenous SP-A treatment (Figure 4A), suggesting that AMs had developed to not overreact to SP-A exposure during their development and maturation in the pulmonary environment. The *in vivo* results also suggest that SP-A activated NK cells to demonstrate antitumor activity; however, exogenous treatment of SP-A did not directly affect Prf1 or GzmB gene expression in NK cells *in vitro* (Figure 4D). These results suggest that SP-A activated and attracted circulating monocytes/macrophages to obtain the M1 phenotype and that these increased M1 TAMs then recruited and activated NK cells to exhibit cell killing.

Effect of SP-A on the Lung Cancer Metastasis Model *in Vivo*

We next examined the effect of SP-A on lung metastasis induced by lung cancer cells. Intravenous injection of PC14PE6 or A549 cells into nude mice lead to the development of metastatic colonies in the lung. In addition, mice injected with PC14PE6 developed a large volume of pleural effusion.[17,18] We compared the number of lung metastatic colonies, lung weight, and the amount of pleural effusion produced by vector control and SP-A–expressing cells. Mice injected with PC14PE6/SP-A cells produced significantly fewer lung metastatic colonies and a lower amount of pleural effusion than those injected with vector control cells (Table 2 and Figure 5A). Similarly, the lung metastasis formed by A549 cells was also suppressed by SP-A expression. Analogous to the results we obtained in the xenograft experiments, the numbers of CD68-positive macrophages, M1 macrophages, and NK cells were increased in the SP-A–expressing metastatic tumors compared with vector controls (Figure 5, B and C). The expression of multiple M1 markers, as well as Prf1 and GzmB, was up-regulated in the lung metastatic colonies formed by PC14PE6/SP-A, whereas the expression of M2 markers was not changed (Figure 5D).

Importance of NK Cells in the SP-A–Mediated Antitumor Effect in Lung Cancer Metastasis

To confirm that the activation of NK cells was essential in the antitumor effect of SP-A, we performed a lung metastasis experiment using nude mice depleted of NK cells.[19] As shown in Table 3 and Figure 5E, PC14PE6/SP-A cells were confirmed to produce significantly fewer lung metastatic colonies and a lower volume of pleural effusion compared with control cells when injected into NK^+ nude mice. However, when NK cells were depleted, no difference was observed in lung metastasis between PC14PE6/SP-A and control cells. These results indicate that the activation of NK cells was essential for SP-A–mediated suppression of lung cancer progression. Taken together, these findings suggest

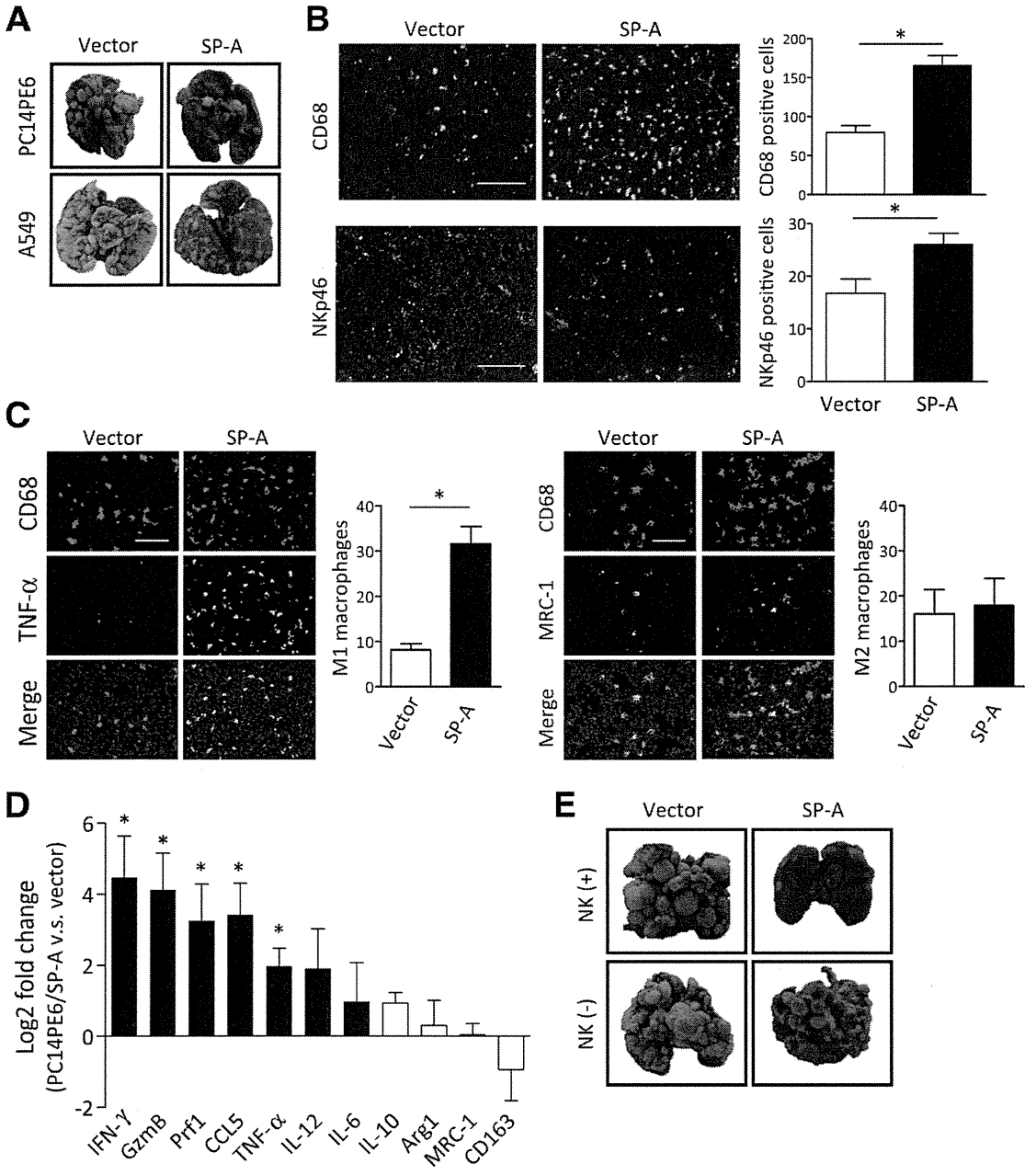

Figure 5 The effect of SP-A on lung cancer metastasis. **A**: Representative images of lung metastasis produced by SP-A– or vector-transduced lung cancer cell lines. **B**: IF staining of CD68 or NKp46. Nuclei were counterstained with DAPI (blue). **C**: IF double staining of CD68 (red) and TNF-α (green) or MRC-1 (green) in PC14PE6 lung metastasis. **D**: Gene expression of mouse M1 and M2 markers in PC14PE6 metastatic lung nodules determined by RT-PCR. The increased gene expression in PC14PE6/SP-A compared with control (vector) is shown as $\log_2$-fold changes. Data are the average of four to five mice per group. IFN-γ, interferon γ. **E**: Representative images of the lung metastasis formed by PC14PE6/SP-A or vector in nude mice (NK^+) or NK cell–depleted nude mice (NK^-). Data are presented as means ± SEM. $^*P < 0.05$. Scale bars: 200 μm (**B**); 100 μm (**C**).

that SP-A in the tumor microenvironment displays anti-tumor activity by mediating the polarization of TAMs toward an M1-dominant phenotype, which, in turn, activates NK cells that then limit tumor progression.

Discussion

In this study, we demonstrated that i) SP-A expression in cancer cells suppresses progression of lung adenocarcinoma in xenograft and lung metastasis models; ii) SP-A inhibits lung cancer progression not by its direct effect on tumor cells but by regulating the host microenvironment, including macrophages and NK cells; and iii) SP-A increases the number of M1 TAMs in the tumor microenvironment, resulting in NK cell recruitment and activation in tumor tissue. These results suggest new immunoregulatory functions of SP-A, which is frequently expressed in pulmonary adenocarcinoma.

Tumors comprise not only malignant cells but also many other nonmalignant cell types, and they produce a unique

Table 3 Effect of SP-A on Lung Metastasis Produced by PC14PE6 Cells in Nude Mice Depleted of NK Cells

	Lung			Pleural effusion	
		Metastasis			
PC14PE6	Weight (g)	Incidence	No.	Incidence	Volume (μL)
Vector NK^+	0.41 (0.24–0.65)	6/6	113.0 (35–197)	6/6	313.3 (20–900)
SP-A NK^+	0.21 (0.15–0.26)*	5/5	25.6 (6–34)*	1/5	80.0 (0–400)
Vector NK^-	0.50 (0.26–0.89)	7/7	148.6 (52–207)	7/7	438.6 (20–1000)
SP-A NK^-	0.34 (0.21–0.48)	5/5	101.2 (41–181)	4/5	400.0 (0–1200)

PC14PE6 cells were i.v. injected into nude mice with or without NK cell depletion, and lung metastasis and pleural effusion were evaluated. Values are means (ranges).

*Statistically significant difference compared with vector NK^+ ($P < 0.05$).

microenvironment that can modify the neoplastic properties of the tumor cells. Among the cells recruited in the tumor microenvironment, TAMs are one of the major players known to have pivotal roles in the progression and metastasis of tumors.[23,24] Although partially contradictive, high numbers of TAMs often correlate with poor prognosis in various types of cancer.[28] Therefore, a better understanding of the role of TAMs seems crucial to control cancer progression.

Considering the character of TAMs, it is now generally accepted that TAMs usually polarize to M2 and represent protumoral functions.[23] Indeed, we have seen in this study that approximately 60% of TAMs had the M2 phenotype in PC14PE6 and A549 control (vector-transduced) tumors (Figures 2B and 5C). However, when tumor cells expressed SP-A, this M1/M2 balance was reversed, and M1 macrophages became dominant in both tumors. As far as we have investigated, the expression of multiple M1 markers was upregulated in SP-A–expressing tumors, whereas the expression of M2 markers was not altered in xenograft and metastatic lung tumors. Together with the fact that the number of M1 TAMs was increased in SP-A–expressing tumors, these results indicate that SP-A aided in making the TAMs M1 dominant by increasing the number of recruited M1 macrophages rather than shifting the M2 TAMs into the M1 phenotype in the tumor microenvironment.

Numerous studies have shown that macrophages could be a target cell type that SP-A interacts with to regulate infectious inflammation, and, to date, diverse and contradictive functions of SP-A against monocytes/macrophages are reported.[29–32] These studies all indicate that SP-A has various effects on inflammation induced by different agonists. Indeed, we also observed that the cytokine/chemokine expression profiles of PMs and human monocytes were different in response to SP-A (Figure 4), suggesting that SP-A may exert cell- and agonist-specific effects that contribute to the inflammation state of the host.

In addition to the observations investigating the role of SP-A during infection, we showed that SP-A activates and increases M1 macrophages in the tumor microenvironment and induces the production of inflammatory cytokines, suggesting that SP-A facilitates inflammation in the tumor to reduce tumor progression. The precise molecular mechanism by which SP-A activates M1 macrophages in the tumor remains unclear with the current observation; however, several mechanisms should be considered. First, SP-A may enhance the binding of cytokines to their respective receptors. SP-A is reported to bind to several receptors, including Toll-like receptors 2 and 4, and to regulate inflammatory responses induced by pathogen-derived products, such as peptidoglycan and lipopolysaccharide via Toll-like receptors.[33–35] In addition to its role in Toll-like receptor–mediated cellular responses induced by infectious challenges, it is very possible that SP-A regulates the function of TAMs in the tumor microenvironment through the interaction with Toll-like receptors. Second, signal transduction in the TAMs could be regulated by SP-A. SP-A has been shown to trigger rapid tyrosine, but not serine or threonine, phosphorylation[36] of macrophage proteins and could possibly enhance/accelerate the initial phosphorylation steps of the signal transduction pathway, which leads to the regulation of inflammation in the tumor. It was also possible that SP-A directly affects tumor cells and regulates cytokine expression. Thus, we compared the chemokine expression of SP-A–expressing PC14PE6 and control (vector-transduced) cells using the PCR array system. Of 92 chemokine and chemokine-related genes tested, none were altered by SP-A overexpression (data not shown), suggesting that SP-A did not directly affect chemokine expression of tumor cells.

Of note, we showed the effect of SP-A on M1 macrophage recruitment and tumor suppression in xenograft and lung metastasis models. This result indicated two important aspects of SP-A. First, the lung tumor–specific expression of SP-A is more important than the host SP-A in the lung to suppress lung cancer progression. Second, the recruited M1 TAMs by tumor-derived SP-A could be originated from circulating monocytes. This possibility was supported by the result that SP-A activated only circulating monocytes/macrophages (mouse PMs or human monocytes) and showed no effect on resident AMs in cytokine expression. In the lung, the sensitivity of resident AMs against SP-A is thought to be suppressed as they are continuously contacted by SP-A, which could be a plausible explanation because the host needs to be protected from the overzealous inflammation in the resting, normal, noninflamed lungs. The molecular mechanism of different SP-A sensitivities in different cells is

not still clearly understood. However, as stated previously herein, the expression of inflammatory signaling molecules that might be regulated by SP-A could be different between AMs and other type of monocytes/macrophages. In addition, there could be an unknown SP-A receptor(s) that might be critical in regulating inflammation in macrophages, as SP-A is reported to bind to multiple receptors.[2] Further studies are needed to understand the precise molecular mechanisms of the diverse and cell-specific function of SP-A against macrophages in the context of SP-A and lung cancer.

These results indicate that NK cell activation was the main mechanism by which SP-A lead to the reduction in tumor burden. The production of Prf1 and GzmB was strongly increased (15- to 30-fold), whereas the number of NK cells was increased only twofold to threefold in the SP-A–expressing tumor, suggesting the multiple pathways regulated by SP-A to recruit and activate NK cells. Because cytokines produced by M1 macrophages, such as interferon-γ and CCL2, are known to activate NK cells,[37–39] it is likely that SP-A implicitly induces NK cell killing via activating M1 TAMs and increasing various inflammatory cytokines in the tumor microenvironment.

Two functional genes of SP-A were detected in a previous report[40]: SP-A1 and SP-A2. These genes were differentially regulated by development[41] and have a minor difference in carbohydrate-binding activity.[42] However, SP-A protein derived from SP-A1 and SP-A2 genes are reported to be functional and to enhance TNF-α secretion by the monocytic cell line.[43] Thus, although we have transduced only the SP-A1 gene, we suspect that SP-A protein from the SP-A2 gene could also contribute to activation of the innate immune system and suppress tumor progression.

In conclusion, these findings demonstrate that SP-A regulates the tumor microenvironment by controlling the polarization of TAMs. SP-A expression by tumor cells leads to increased numbers and the activation of M1 TAMs. These activated M1 TAMs then recruit and activate NK cells that function in tumor suppression. These results indicate that SP-A plays an important protective role in the progression of lung cancer. Specifically targeting M1 TAMs (not bulk TAMs) to induce the activation of a proinflammatory program in the tumor, generating the pharmacologic modulators of SP-A for example, could be the therapeutic approach to improve the effect of anticancer therapy.

Acknowledgments

This work was performed in collaboration with the late Dr. Jo Rae Wright (Duke University, Durham, NC). We greatly appreciate and honor her contribution to this work.

We also thank Kathy Evans (Duke University) for the preparation of purified human SP-A, Tomoko Oka and the Support Center for Advanced Medical Sciences (The University of Tokushima) for technical assistance, and the Student Lab (The University of Tokushima) for helpful discussions.

Supplemental Data

Supplemental material for this article can be found at *http://dx.doi.org/10.1016/j.ajpath.2013.01.030.*

References

1. Jemal A, Siegel R, Ward E, Hao Y, Xu J, Thun MJ: Cancer statistics, 2009. CA Cancer J Clin 2009, 59:225–249
2. Wright JR: Immunoregulatory functions of surfactant proteins. Nat Rev Immunol 2005, 5:58–68
3. Borron P, McIntosh JC, Korfhagen TR, Whitsett JA, Taylor J, Wright JR: Surfactant-associated protein A inhibits LPS-induced cytokine and nitric oxide production in vivo. Am J Physiol Lung Cell Mol Physiol 2000, 278:840–847
4. LeVine AM, Gwozdz J, Stark J, Bruno M, Whitsett J, Korfhagen T: Surfactant protein-A enhances respiratory syncytial virus clearance in vivo. J Clin Invest 1999, 103:1015–1021
5. Mariencheck WI, Savov J, Dong Q, Tino MJ, Wright JR: Surfactant protein A enhances alveolar macrophage phagocytosis of a live, mucoid strain of P. aeruginosa. Am J Physiol 1999, 277:777–786
6. Giannoni E, Sawa T, Allen L, Wiener-Kronish J, Hawgood S: Surfactant proteins A and D enhance pulmonary clearance of Pseudomonas aeruginosa. Am J Respir Cell Mol Biol 2006, 34:704–710
7. Atochina EN, Beck JM, Preston AM, Haczku A, Tomer Y, Scanlon ST, Fusaro T, Casey J, Hawgood S, Gow AJ, Beers MF: Enhanced lung injury and delayed clearance of Pneumocystis carinii in surfactant protein A-deficient mice: attenuation of cytokine responses and reactive oxygen-nitrogen species. Infect Immun 2004, 72: 6002–6011
8. Kuronuma K, Sano H, Kato K, Kudo K, Hyakushima N, Yokota S, Takahashi H, Suzuki H, Kodama T, Abe S, Kuroki Y: Pulmonary surfactant protein A augments the phagocytosis of Streptococcus pneumoniae by alveolar macrophages through a casein kinase 2-dependent increase of cell surface localization of scavenger receptor A. J Biol Chem 2004, 279:21421–21430
9. Goto H, Ledford JG, Mukherjee S, Noble PW, Williams KL, Wright JR: The role of surfactant protein A in bleomycin-induced acute lung injury. Am J Respir Crit Care Med 2010, 181:1336–1344
10. Pastva AM, Walker JK, Maddox LA, Mukherjee S, Giamberardino C, Hsia B, Potts E, Zhu H, Degan S, Sunday ME, Lawson BL, Korfhagen TR, Schwartz DA, Eu JP, Foster WM, McMahon TJ, Que L, Wright JR: Nitric oxide mediates relative airway hyperresponsiveness to lipopolysaccharide in surfactant protein A-deficient mice. Am J Respir Cell Mol Biol 2011, 44:175–184
11. Bejarano PA, Baughman RP, Biddinger PW, Miller MA, Fenoglio-Preiser C, al-Kafaji B, Di Lauro R, Whitsett JA: Surfactant proteins and thyroid transcription factor-1 in pulmonary and breast carcinomas. Mod Pathol 1996, 9:445–452
12. Jiang F, Caraway NP, Nebiyou Bekele B, Zhang HZ, Khanna A, Wang H, Li R, Fernandez RL, Zaidi TM, Johnston DA, Katz RL: Surfactant protein A gene deletion and prognostics for patients with stage I non-small cell lung cancer. Clin Cancer Res 2005, 11: 5417–5424
13. Tsutsumida H, Goto M, Kitajima S, Kubota I, Hirotsu Y, Yonezawa S: Combined status of MUC1 mucin and surfactant apoprotein A expression can predict the outcome of patients with small-size lung adenocarcinoma. Histopathology 2004, 44:147–155
14. McIntosh JC, Swyers AH, Fisher JH, Wright JR: Surfactant proteins A and D increase in response to intratracheal lipopolysaccharide. Am J Respir Cell Mol Biol 1996, 15:509–519
15. Morita S, Kojima T, Kitamura T: Plat-E: an efficient and stable system for transient packaging of retroviruses. Gene Ther 2000, 7:1063–1066
16. Maekawa S, Tsukumo S, Chiba S, Hirai S, Hayashi Y, Okada H, Kishihara K, Yasutomo K: Delta1-Notch3 interactions bias the

functional differentiation of activated CD4+ T cells. Immunity 2003, 19:549–559
17. Yano S, Nokihara H, Yamamoto A, Goto H, Ogawa H, Kanematsu T, Miki T, Uehara H, Saijo Y, Nukiwa T, Sone S: Multifunctional interleukin-1β promotes metastasis of human lung cancer cells in SCID mice via enhanced expression of adhesion-, invasion- and angiogenesis-related molecules. Cancer Sci 2003, 94:244–252
18. Yano S, Shinohara H, Herbst RS, Kuniyasu H, Bucana CD, Ellis LM, Fidler IJ: Production of experimental malignant pleural effusions is dependent on invasion of the pleura and expression of vascular endothelial growth factor/vascular permeability factor by human lung cancer cells. Am J Pathol 2000, 157:1893–1903
19. Yano S, Nishioka Y, Izumi K, Tsuruo T, Tanaka T, Miyasaka M, Sone S: Novel metastasis model of human lung cancer in SCID mice depleted of NK cells. Int J Cancer 1996, 67:211–217
20. de Jonge HJ, Fehrmann RS, de Bont ES, Hofstra RM, Gerbens F, Kamps WA, de Vries EG, van der Zee AG, te Meerman GJ, ter Elst A: Evidence based selection of housekeeping genes. PLoS One 2007, 2:898
21. Utsugi T, Sone S: Comparative analysis of the priming effect of human interferon-gamma, -alpha, and -beta on synergism with muramyl dipeptide analog for anti-tumor expression of human blood monocytes. J Immunol 1986, 136:1117–1122
22. Hyodo Y, Matsui K, Hayashi N, Tsutsui H, Kashiwamura S, Yamauchi H, Hiroishi K, Takeda K, Tagawa Y, Iwakura Y, Kayagaki N, Kurimoto M, Okamura H, Hada T, Yagita H, Akira S, Nakanishi K, Higashino K: IL-18 up-regulates perforin-mediated NK activity without increasing perforin messenger RNA expression by binding to constitutively expressed IL-18 receptor. J Immunol 1999, 162:1662–1668
23. Pollard JW: Tumour-educated macrophages promote tumour progression and metastasis. Nat Rev Cancer 2004, 4:71–78
24. Solinas G, Germano G, Mantovani A, Allavena P: Tumor-associated macrophages (TAM) as major players of the cancer-related inflammation. J Leukoc Biol 2009, 86:1065–1073
25. Benoit M, Desnues B, Mege JL: Macrophage polarization in bacterial infections. J Immunol 2008, 181:3733–3739
26. Robertson MJ: Role of chemokines in the biology of natural killer cells. J Leukoc Biol 2002, 71:173–183
27. Langers I, Renoux VM, Thirty M, Delvenne P, Jacobs N: Natural killer cells: role in local growth and metastasis. Biologics 2012, 6:73–82
28. Bingle L, Brown NJ, Lewis CE: The role of tumour-associated macrophages in tumour progression: implications for new anticancer therapies. J Pathol 2002, 196:254–265
29. Kremlev SG, Phelps DS: Surfactant protein A stimulation of inflammatory cytokine and immunoglobulin production. Am J Physiol 1994, 267:712–719
30. Kremlev SG, Umstead TM, Phelps DS: Surfactant protein A regulates cytokine production in the monocytic cell line THP-1. Am J Physiol 1997, 272:996–1004
31. McIntosh JC, Mervin-Blake S, Conner E, Wright JR: Surfactant protein A protects growing cells and reduces TNF-alpha activity from LPS-stimulated macrophages. Am J Physiol 1996, 271:310–319
32. Stamme C, Walsh E, Wright JR: Surfactant protein A differentially regulates IFN-gamma- and LPS-induced nitrite production by rat alveolar macrophages. Am J Respir Cell Mol Biol 2000, 23:772–779
33. Sano H, Sohma H, Muta T, Nomura S, Voelker DR, Kuroki Y: Pulmonary surfactant protein A modulates the cellular response to smooth and rough lipopolysaccharides by interaction with CD14. J Immunol 1999, 163:387–395
34. Sato M, Sano H, Iwaki D, Kudo K, Konishi M, Takahashi H, Takahashi T, Imaizumi H, Asai Y, Kuroki Y: Direct binding of Toll-like receptor 2 to zymosan, and zymosan-induced NF-kappa B activation and TNF-alpha secretion are down-regulated by lung collectin surfactant protein A. J Immunol 2003, 171:417–425
35. Henning LN, Azad AK, Parsa KV, Crowther JE, Tridandapani S, Schlesinger LS: Pulmonary surfactant protein A regulates TLR expression and activity in human macrophages. J Immunol 2008, 180: 7847–7858
36. Schagat TL, Tino MJ, Wright JR: Regulation of protein phosphorylation and pathogen phagocytosis by surfactant protein A. Infect Immun 1999, 67:4693–4699
37. Rolny C, Mazzone M, Tugues S, Laoui D, Johansson I, Coulon C, Squadrito ML, Segura I, Li X, Knevels E, Costa S, Vinckier S, Dresselaer T, Akerud P, De Mol M, Salomaki H, Phillipson M, Wyns S, Larsson E, Buysschaert I, Botling J, Himmelreich U, Van Ginderachter JA, De Palma M, Dewerchin M, Claesson-Welsh L, Carmeliet P: HRG inhibits tumor growth and metastasis by inducing macrophage polarization and vessel normalization through down-regulation of PlGF. Cancer Cell 2011, 19:31–44
38. Schroder K, Hertzog PJ, Ravasi T, Hume DA: Interferon-gamma: an overview of signals, mechanisms and functions. J Leukoc Biol 2004, 75:163–189
39. Morrison BE, Park SJ, Mooney JM, Mehrad B: Chemokine-mediated recruitment of NK cells is a crucial host defense mechanisms in invasive aspergillosis. J Clin Invest 2003, 112:1862–1870
40. White RT, Damm D, Miller J, Spratt K, Schilling J, Hawgood S, Benson B, Cordell B: Isolation and characterization of the human pulmonary surfactant apoprotein gene. Nature 1985, 317:361–363
41. McCormick SM, Mendelson CR: Human SP-A1 and SP-A2 genes are differentially regulated during development and by cAMP and glucocorticoids. Am J Physiol 1994, 266:367–374
42. Oberley RE, Snyder JM: Recombinant human SP-A1 and SP-A2 proteins have different carbohydrate-binding characteristics. Am J Physiol Lung Cell Mol Physiol 2003, 284:871–881
43. Wang G, Phelps DS, Umstead TM, Floros J: Human SP-A protein variants derived from one or both genes stimulate TNF-alpha production in the THP-1 cell line. Am J Physiol Lung Cell Mol Physiol 2000, 278:946–954

J. Biochem. 2012;151(2):205–216 doi:10.1093/jb/mvr136

JB THE JOURNAL OF BIOCHEMISTRY

TGF-β-induced epithelial-mesenchymal transition of A549 lung adenocarcinoma cells is enhanced by pro-inflammatory cytokines derived from RAW 264.7 macrophage cells

Received August 23, 2011; accepted November 21, 2011; published online December 7, 2011

Mikiko Kawata[1], Daizo Koinuma[1], Tomohiro Ogami[1], Kazuo Umezawa[2], Caname Iwata[1], Tetsuro Watabe[1] and Kohei Miyazono[1,*]

[1]Department of Molecular Pathology, Graduate School of Medicine, University of Tokyo, Hongo 7-3-1, Bunkyo-ku, Tokyo 113-0033; and [2]Faculty of Science and Technology, Keio University, Yokohama 223-0061, Japan

*Kohei Miyazono, Department of Molecular Pathology, Graduate School of Medicine, University of Tokyo, Hongo 7-3-1, Bunkyo-ku, Tokyo 113-0033, Japan. Tel: +81-3-5841-3356, Fax: +81-3-5841-3354, email: miyazono@m.u-tokyo.ac.jp

Cancer cells undergo epithelial-mesenchymal transition (EMT) during invasion and metastasis. Although transforming growth factor-β (TGF-β) and pro-inflammatory cytokines have been implicated in EMT, the underlying molecular mechanisms remain to be elucidated. Here, we studied the effects of proinflammatory cytokines derived from the mouse macrophage cell line RAW 264.7 on TGF-β-induced EMT in A549 lung cancer cells. Co-culture and treatment with conditioned medium of RAW 264.7 cells enhanced a subset of TGF-β-induced EMT phenotypes in A549 cells, including changes in cell morphology and induction of mesenchymal marker expression. These effects were increased by the treatment of RAW 264.7 cells with lipopolysaccharide, which also induced the expression of various proinflammatory cytokines, including TNF-α and IL-1β. The effects of conditioned medium of RAW 264.7 cells were partially inhibited by a TNF-α neutralizing antibody. Dehydroxy methyl epoxyquinomicin, a selective inhibitor of NFκB, partially inhibited the enhancement of fibronectin expression by TGF-β, TNF-α, and IL-1β, but not of N-cadherin expression. Effects of other pharmacological inhibitors also suggested complex regulatory mechanisms of the TGF-β-induced EMT phenotype by TNF-α stimulation. These findings provide direct evidence of the effects of RAW 264.7-derived TNF-α on TGF-β-induced EMT in A549 cells, which is transduced in part by NFκB signalling.

Keywords: EMT/lung adenocarcinoma/NFκB/TGF-β/TNF-α.

Abbreviations: δEF1, delta-crystallin/E2-box factor 1; DHMEQ, dehydroxy methyl epoxyquinomicin; EMT, epithelial-mesenchymal transition; GAPDH, glyceraldehyde-3-phosphate dehydrogenase; HMGA2, high mobility group AT-hook 2; ICAM-1, intercellular adhesion molecule-1; Id, inhibitor of differentiation; IL, interleukin; LPS, lipopolysaccharide; MMP, matrix metalloproteinase; NFκB, nuclear factor kappa-light-chain-enhancer of activated B cells; RT, reverse transcription; SIP1, Smad interacting protein-1; siRNA, small interfering RNA; TβR, TGF-β receptor; TGF-β, transforming growth factor-β; TNF-α, tumour necrosis factor-α; TTF-1, thyroid transcription factor-1.

Cytokines of the transforming growth factor-β (TGF-β) family have multiple roles in development and diseases (*1–3*). TGF-β inhibits the proliferation of normal epithelial cells, but cancer cells often evade this control. Furthermore, TGF-β induces epithelial–mesenchymal transition (EMT) in cancer cells, enabling the cells to become motile and invasive (*2*, *4–7*). Since cancer cells are subjected to numerous extracellular stimulations *in vivo*, elucidating the roles of these factors on TGF-β-induced EMT is important for developing cancer treatments.

TGF-β binds to the TGF-β type II receptor (TβRII) on the cell membrane, forming a complex with the type I TGF-β receptor (TβRI) and activating it by phosphorylation (*8*, *9*). The intracellular signalling pathway of the TGF-β family is primarily induced by Smad family proteins. The receptor complex phosphorylates Smad2 and Smad3 on their C-terminal SSXS motifs, resulting in hetero-oligomer formation with Smad4, followed by translocation to the nucleus where they act as transcription factors.

The mechanism of TGF-β-induced EMT has been intensively examined, and each phenotype of EMT was found to be regulated by distinct regulatory factors. For example, expression of E-cadherin mRNA was suppressed by TGF-β via the induction of transcription factors Snail, Slug, high-mobility group AT-hook 2 (HMGA2), delta-crystallin/E2-box factor 1 (δEF1) and Smad interacting protein-1 (SIP1) (*10*, *11*). E12/E47 also represses E-cadherin when inhibitor of differentiation (Id) proteins are downregulated by TGF-β (*12*). Complex formation between Smads and Snail has been reported to be important for E-cadherin regulation by TGF-β (*13*). In contrast, the regulatory mechanisms involved in the expression of mesenchymal markers fibronectin and N-cadherin is poorly understood, and is generally not regulated by the

above factors (*11*, *14*). Induction of α-smooth muscle actin by TGF-β is reported to be induced by nuclear translocation of myocardin family proteins (*15*, *16*). We previously found that thyroid transcription factor-1 (TTF-1) is expressed in the lung epithelium and inhibits TGF-β-induced EMT in A549 lung adenocarcinoma cells, suggesting that TTF-1 is an intrinsic inhibitor of TGF-β-induced EMT (*17*).

Extracellular signals other than TGF-β have been shown to induce EMT in a variety of cells with or without the cooperation of TGF-β (*18*). FGF-2 cooperates with TGF-β to induce EMT and promotes invasion of cancer (*19*). Recent reports have suggested that inflammation plays an important role in tumour progression. Inflammatory cells in the tumour micro-environment produce various inflammatory cytokines, which are involved in the EMT of cancer cells. Previous reports have shown that various pro-inflammatory cytokines, including tumour necrosis factor-α (TNF-α), are produced from activated macrophages (*20*), and that these cytokines augment TGF-β-induced EMT in A549 cells (*21*), whereas TNF-α by itself does not induce EMT in A549 cells (*22*). However, the roles of macrophage-derived inflammatory cytokines in TGF-β-induced EMT of lung cancer cells and the molecular mechanisms underlying this process are not fully understood.

In the present study, we examined the effect of factors derived from a mouse macrophage cell line RAW 264.7 on TGF-β-induced EMT in A549 cells. We found that RAW 264.7-derived factors enhance some phenotypes of TGF-β-induced EMT in A549 cells, including upregulation of fibronectin and N-cadherin. We also showed that the effects of conditioned medium of RAW 264.7 cells on TGF-β-induced EMT is inhibited by a neutralizing antibody against TNF-α, suggesting that the secretion of TNF-α from RAW 264.7 cells is critical for TGF-β-induced EMT. We further found that interleukin (IL)-1β is produced by RAW 264.7 cells and augments TGF-β-induced EMT in A549 cells. Interestingly, the effect is partially mediated by nuclear factor kappa-light-chain-enhancer of activated B cells (NFκB) signalling which is suppressed by a specific inhibitor dehydroxy methyl epoxyquinomicin (DHMEQ). Effects of other pharmacological inhibitors on enhancement of TGF-β-induced EMT by TNF-α and IL-1β were also evaluated. Our findings suggest that TNF-α and IL-1β endogenously secreted from RAW 264.7 cells enhance TGF-β-induced EMT in A549 cells at least in part through NFκB signalling.

Materials and Methods

Cell culture and reagents

RAW 264.7, a macrophage-like cell line established from an ascites of tumour induced in mouse by intraperitoneal injection of Abelson leukaemia virus, was a kind gift from Dr Tadashi Muroi (NIH Sciences). A549 and RAW264.7 cells were maintained in Dulbecco's modified Eagle's medium (DMEM) (GIBCO/Life Technologies, Carlsbad, CA, USA) supplemented with 10% fetal bovine serum (FBS), 100 U/ml of penicillin G and 100 μg/ml of streptomycin. NMuMG cells were cultured in DMEM supplemented with 10% FBS, 100 U/ml of penicillin G, 100 μg/ml of streptomycin and 10 μg/ml of insulin. Cells were grown in a 5% CO_2 atmosphere at 37°C. Recombinant human TGF-β1, TNF-α and IL-1β were obtained from R&D Systems (Minneapolis, MN, USA). Recombinant human IL-6 was purchased from Peprotech (Rocky Hill, NJ, USA). Lipopolysaccharide (LPS) was from SIGMA (St Louis, MO, USA) and GM6001, a pan-matrix metalloproteinase (MMP) inhibitor, was from Calbiochem (San Diego, CA, USA). DHMEQ has been described previously (*23*, *24*). U0126 was from Promega (Fitchburg, WI, USA). SP600125 and SB203580 were from Calbiochem.

Preparation of conditioned medium of RAW 264.7 cells

RAW 264.7 cells (4.5×10^6) were cultured in 10 ml growth medium in a 100-mm dish with or without LPS for 24 h. A549 cells were pre-cultured in a 6-well plate for 24 h with or without TGF-β. Culture medium was replaced with 2 ml/well of the obtained conditioned medium containing TGF-β where indicated.

Quantitative reverse transcription polymerase chain reaction

Total RNAs were extracted using the RNeasy Mini Kit (QIAGEN, Hilden, Germany) as described previously (*25*). First-strand cDNAs were synthesized using the SuperScript III First-Strand Synthesis System (Life Technologies). Quantitative real-time PCR (qRT–PCR) analysis was performed as described previously (*25*). Amplification data were quantified using the standard curve method. All samples were run in duplicate, and the results were averaged and normalized to expression of glyceraldehyde-3-phosphate dehydrogenase (GAPDH). Primer sequences are available as Supplementary Table I.

Immunoblotting

A549 cells were washed with PBS and lysed with Radioimmunoprecipitation assay buffer [20 mM Tris–HCl (pH 7.5), 150 mM NaCl, 10 mM EDTA, 1 mM EGTA, 1% Nonidet P-40, 0.5% sodium deoxycholate, 0.1% SDS] or cell lysis buffer containing 0.5% Nonidet P-40, 20 mM Tris–HCl (pH 8.0), 150 mM NaCl, 5 mM EDTA, 1 mM phenylmethylsulphonyl fluoride and 10 mg/ml aprotinin (*26*, *27*). SDS polyacrylamide gel-electrophoresis (SDS–PAGE) and immunodetection were performed as described previously (*28*). Antibodies used for immunoblotting included anti-fibronectin (SIGMA), anti-N-cadherin (BD Biosciences, San Jose, CA, USA), anti-E-cadherin (BD), anti-α-tubulin (SIGMA) and anti-phospho-Smad2 (Cell Signaling Technology, Danvers, MA, USA).

Determination of morphological changes

Morphological changes of the cells were quantitatively determined by calculating cell circularity as described (*29*) by Image J software. Circularity value decreases by morphological change from a pebble-like shape to an elongated shape.

ELISA

Amounts of TNF-α secreted by RAW 264.7 cells were determined in 24 h conditioned media using the Quantikine Mouse TNF-α Immunoassay (R&D Systems), according to the manufacturer's instructions.

Cell invasion assay

Cell invasion assay was performed as described previously with some modifications (*30*). Briefly, cells were pre-treated with or without 5 ng/ml TGF-β and 20 ng/ml TNF-α and seeded in the upper chambers of type-IV collagen-coated (Nitta Gelatin, Osaka, Japan) 12-well culture inserts. After 8 h, cells that had migrated through the collagen-coated-inserts were visualized using crystal violet staining.

Luciferase reporter assays

Luciferase reporter assays were performed as described previously (*31*), by using 9xCAGA-luc (*32*) and NFκB-luc (*33*) as a reporter and TK-Rluc as an internal control.

Neutralizing antibody

Goat anti-mouse TNF-α neutralizing antibody and goat control IgG were obtained from R&D systems. A549 cells were pre-treated with or without 5 ng/ml TGF-β for 24 h, and culture medium was replaced with conditioned medium of RAW 264.7 cells containing either neutralizing antibody or control IgG (10 μg/ml).

Statistical analysis

Student's *t*-test was used to calculate the significance of differences between the two samples. The Tukey–Kramer test of the R statistical analysis programme was used for multiple data comparisons (*34*). A $P<0.05$ was considered to indicate statistical significance.

Results

Secreted factors from RAW 264.7 cells enhance TGF-β-induced EMT of A549 cells

As previously reported (14), TGF-β induces EMT of human lung adenocarcinoma A549 cells that is characterized by morphological changes from a pebble-like shape to an elongated shape (Fig. 1A). These morphological changes were quantitatively determined by the circularity of the cells (*29*) (Fig. 1B). We examined whether secreted factors from mouse RAW 264.7 macrophage cells affect the TGF-β-induced EMT of A549 cells. As shown in Fig. 1A, morphological changes induced by TGF-β were further enhanced by co-culture with RAW 264.7 cells (Fig. 1A and B). To study these effects at a molecular level, qRT–PCR analyses to examine the expression of hallmark EMT genes were performed using human-specific primers. TGF-β-induced expression of the mesenchymal markers fibronectin and N-cadherin were enhanced by the co-culture of the cells (Fig. 1C). Conversely, expression of the epithelial marker E-cadherin was strongly down-regulated by TGF-β, but co-culture of the cells with RAW 264.7 did not elicit an additional effect.

We next determined whether the enhanced EMT was caused by secreted factors from RAW 264.7 cells. Since RAW 264.7 macrophage cells become activated upon treatment with *Escherichia coli*-derived LPS, we examined the effect of conditioned medium of RAW 264.7 cells treated with or without LPS on A549 cells. TGF-β-induced expression of fibronectin and N-cadherin mRNAs was enhanced by the addition of the conditioned medium, which was more significant when the conditioned medium of LPS-treated RAW 264.7 cells was used (Fig. 2A). The effect of the conditioned medium was not observed for repression of E-cadherin by TGF-β, which is in agreement with the

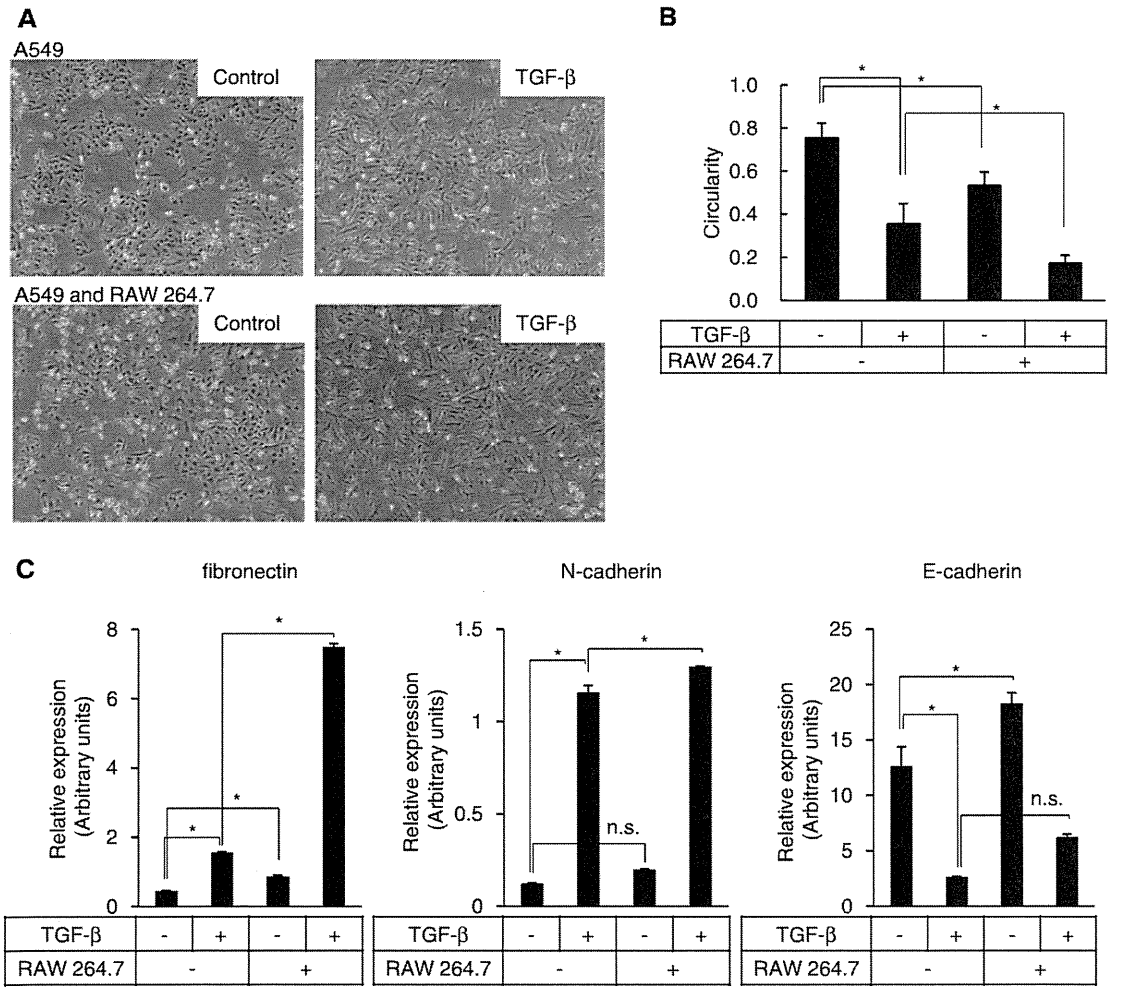

Fig. 1 Effect of co-culture with RAW 264.7 cells on TGF-β-induced EMT of A549 cells. (A) Human lung adenocarcinoma A549 cells were pre-cultured with or without 5 ng/ml TGF-β for 24 h and plated at a density of 5.0×10^4 cells/well in a 6-well plate. The same number of mouse macrophage RAW 264.7 cells were plated and incubated with or without TGF-β for 4 days followed by phase contrast microscopic imaging. (B) Cell circularity was calculated using ImageJ software. In total, 10 cells from each treatment in (A) were measured and the results were averaged. (C) qRT–PCR analysis of EMT marker expression by human-specific primers. A549 cells were co-cultured with RAW 264.7 cells for 3 days with or without TGF-β. $^*P<0.05$; Error bars, SDs; n.s., not significant.

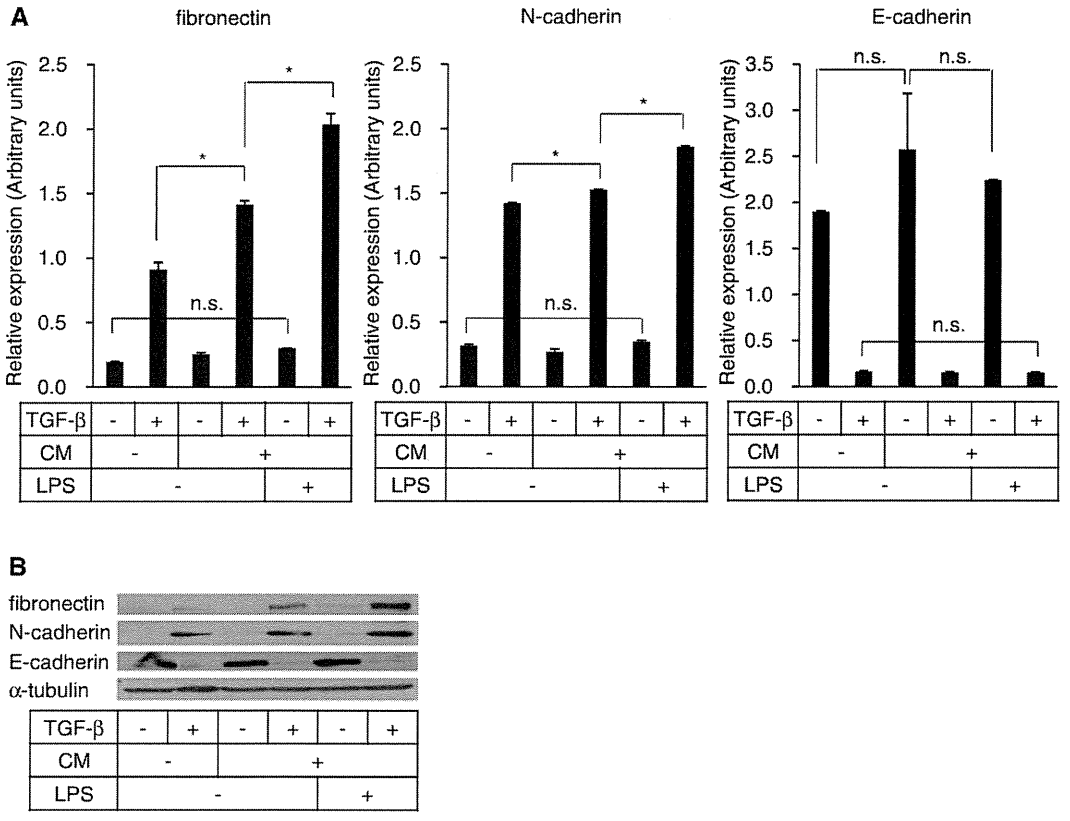

Fig. 2 Effect of conditioned medium of RAW 264.7 cells on TGF-β-induced EMT of A549 cells. (A) A549 cells were cultured with conditioned medium of LPS-activated (0.1 μg/ml) RAW 264.7 cells and stimulated with 5 ng/ml TGF-β. Expression of EMT markers was quantified using qRT–PCR. (B) Expression of fibronectin, N-cadherin and E-cadherin proteins in TGF-β-stimulated A549 cells cultured with conditioned medium of RAW 264.7 cells. A549 cells were cultured as in (A). α-tubulin expression is shown as the loading control. $^*P < 0.05$; CM, conditioned medium; error bars, SDs; n.s., not significant.

results of co-culture assays (Fig. 1C). Of note, treatment of A549 cells with LPS alone did not affect TGF-β-induced EMT phenotypes (Supplementary Fig. 1). The effects of conditioned medium on the expression of fibronectin, N-cadherin and E-cadherin determined using qRT–PCR analysis were confirmed at the protein expression level by immunoblot analysis (Fig. 2B). Secreted factor(s) from activated RAW 264.7 cells therefore enhance EMT of A549 cells stimulated with TGF-β.

TNF-α is secreted from RAW 264.7 cells and enhances TGF-β-induced EMT of A549 cells

We next attempted to identify RAW 264.7-derived factors that enhance the TGF-β-induced EMT in A549 cells. We speculated that production of such factors is increased following treatment of RAW 264.7 cells with LPS. Since TNF-α is reported to be secreted from activated macrophages, we examined the effects of LPS on TNF-α expression in RAW 264.7 cells. We confirmed that TNF-α was expressed in RAW 264.7 cells, which were upregulated following LPS treatment (Fig. 3A). ELISA analysis showed that >600 pg/ml of TNF-α was present in the conditioned medium prepared from the RAW 264.7 cells and that TNF-α concentrations were increased following LPS treatment (Fig. 3B).

When recombinant TNF-α was added to A549 cells, cellular morphology changed both in the absence and presence of TGF-β (Fig. 3C and D). Induction of fibronectin and N-cadherin by TGF-β was also enhanced by TNF-α addition (Fig. 3E). In contrast, E-cadherin expression was strongly suppressed by TGF-β treatment alone and additional effects of TNF-α were not observed. The effects of TNF-α on cellular morphology and mesenchymal marker expression are similar to those observed in the co-culture experiments and those using conditioned medium of RAW 264.7 cells. Notably, E-cadherin expression was not repressed following both co-culture with RAW 264.7 cells and the use of conditioned medium without TGF-β (Fig. 1C and Fig. 2A and B). In contrast, addition of recombinant TNF-α partially inhibited E-cadherin expression without TGF-β stimulation, suggesting that secreted TNF-α was insufficient for effectively regulating E-cadherin expression.

TNF-α enhances TGF-β-induced motility of A549 cells

On the basis of the effect of TNF-α on TGF-β-induced EMT of A549 cells, we next examined its role in cell invasiveness that accompanies with EMT. Cell invasion assay showed that TNF-α enhanced the TGF-β-induced invasion of A549 cells (Fig. 4A). During EMT, MMPs play important roles in stimulating cell invasion. Expression of MMP-9 and MMP-2 was significantly enhanced by TNF-α and TGF-β, but not by TNF-α alone (Fig. 4B). The effect of TNF-α on

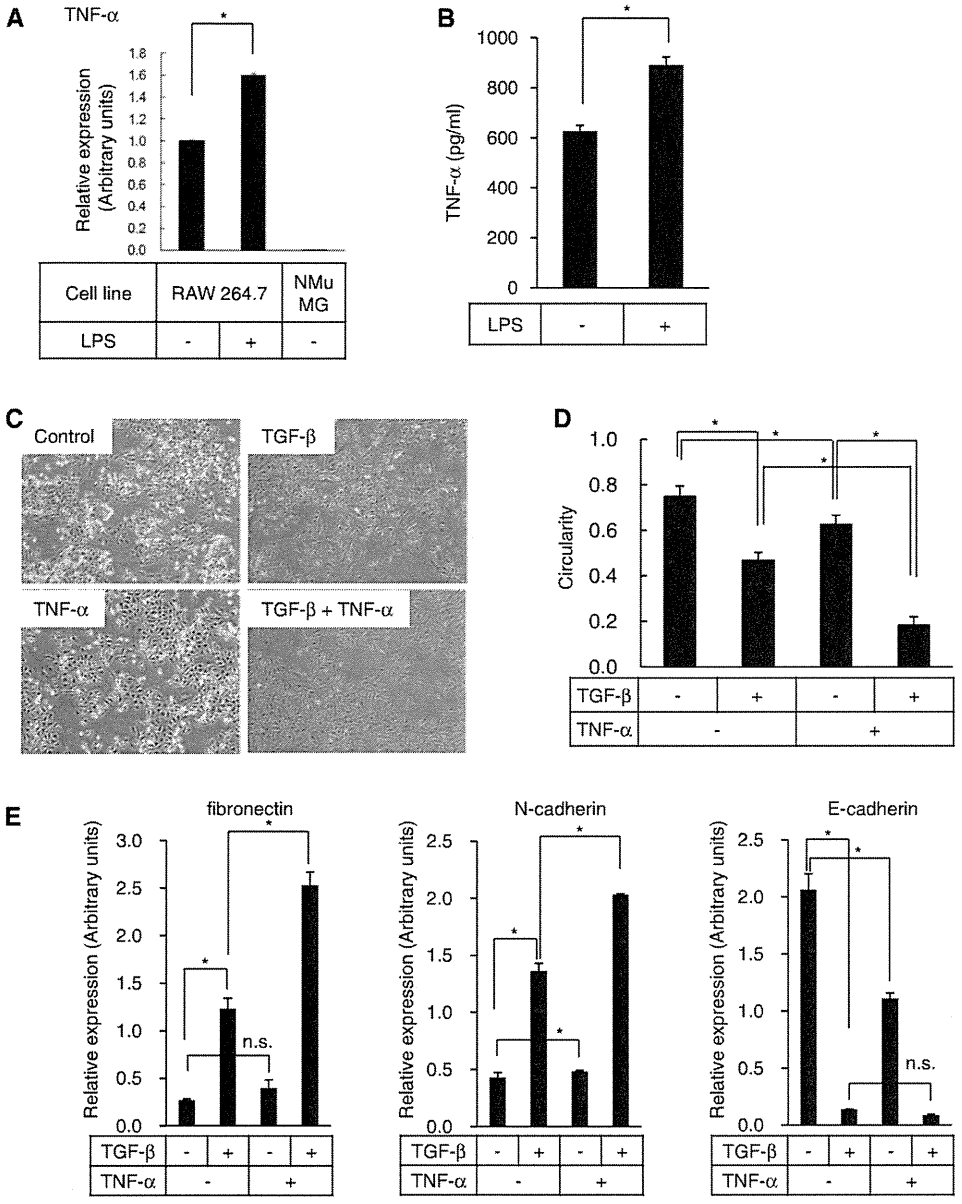

Fig. 3 Enhancement of TGF-β-induced EMT phenotype by TNF-α. (A) Expression of TNF-α mRNA in RAW 264.7 cells. Cells were treated with 0.1 μg/ml LPS, and TNF-α expression was quantified using qRT–PCR. Normal murine mammary gland NMuMG cells served as a negative control. (B) Quantification of secreted TNF-α protein from RAW 264.7 cells stimulated with LPS (0.1 μg/ml). TNF-α protein in the conditioned medium of RAW 264.7 cells was measured using ELISA. (C) Phase-contrast microscopic images of A549 cells treated with 5 ng/ml of TGF-β and 20 ng/ml of TNF-α. Cells were treated with the cytokines for 24 h. (D) Circularity of the cells in (C) was measured as in Fig. 1B. (E) qRT–PCR analysis of EMT marker expression in A549 cells. Cells were treated with 5 ng/ml of TGF-β and 20 ng/ml of TNF-α as indicated for 24 h. $^*P<0.05$; Error bars, SDs; n.s., not significant.

cell invasiveness was dependent in part on MMPs, as shown by the effect of the pan-MMP inhibitor GM6001 (Fig. 4C).

Blocking TNF-α partially abrogates the effects of RAW 264.7-derived factors on the TGF-β-induced EMT in A549 cells

We next evaluated to what extent the effect of conditioned medium of RAW 264.7 cells is attributable to TNF-α by adding anti-mouse TNF-α neutralizing antibody to the conditioned medium of RAW 264.7 cells. When A549 cells were incubated with conditioned medium treated with anti-TNF-α neutralizing antibody, TGF-β-induced expression of fibronectin and N-cadherin was partially suppressed, whereas their basal expression was not significantly affected (Fig. 5). On the basis of these findings, we concluded that TNF-α is secreted from RAW 264.7 cells and enhances the EMT phenotype of A549 cells induced by TGF-β.

IL-1β is produced by RAW 264.7 cells and enhances TGF-β-induced EMT of A549 cells

The observation that anti-TNF-α neutralizing antibody was capable of partially inhibiting the effects of RAW 264.7-derived conditioned medium prompted us

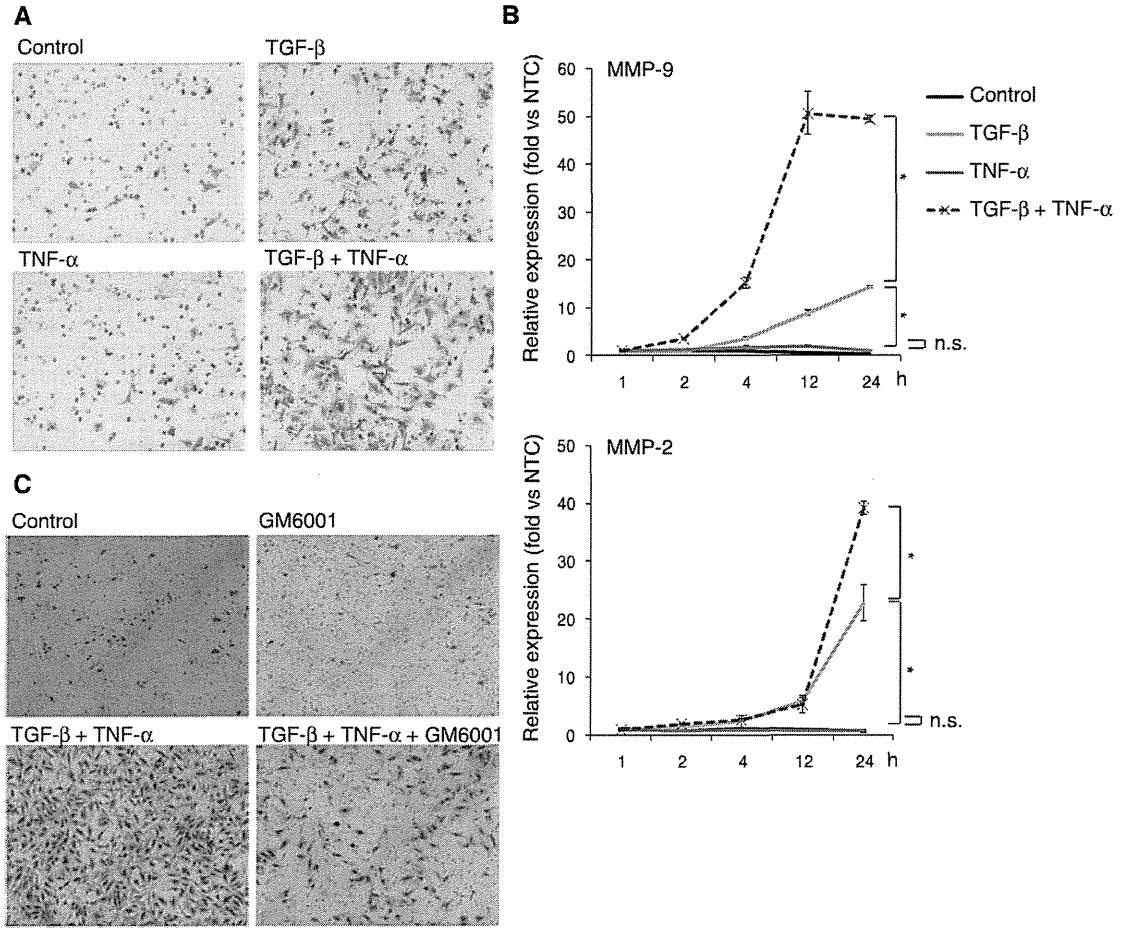

Fig. 4 Effect of TNF-α on the migration A549 cells. (A) Chamber cell invasion assay was performed using A549 cells stimulated with 5 ng/ml TGF-β and 20 ng/ml TNF-α. (B) Expression levels of MMP-2 and MMP-9 in A549 cells treated with TGF-β and TNF-α were analysed using qRT–PCR. (C) Effect of a pan-MMP inhibitor GM6001 on migration of A549 cells. Cells were seeded on Transwells as in (A), and cultured with 10 μM GM6001 in addition to TGF-β and TNF-α for 8 h. NTC, no treatment control at 1 h; $*P<0.05$; Error bars, SDs; n.s., not significant.

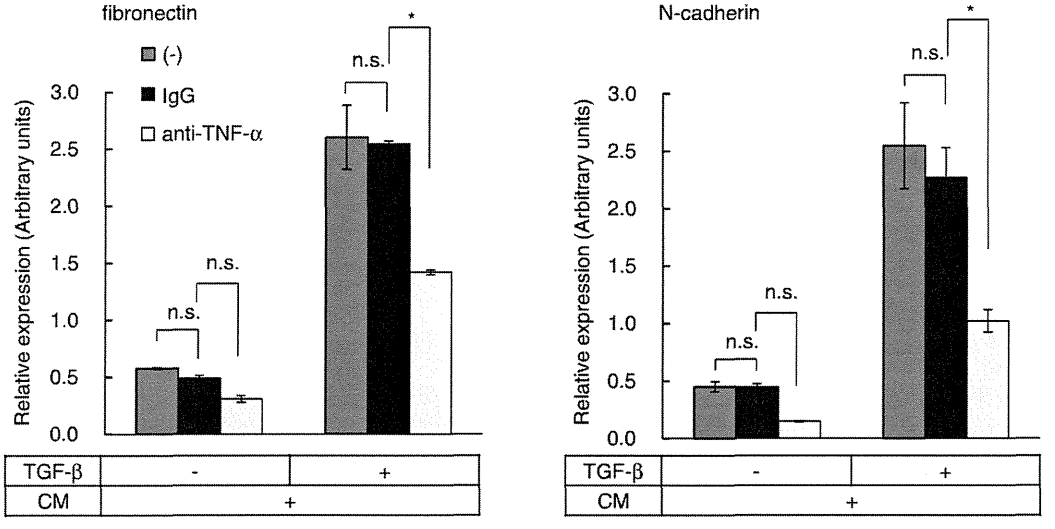

Fig. 5 Effect of TNF-α neutralizing antibody on the expression of mesenchymal markers. A549 cells were cultured in the conditioned medium of RAW 264.7 cells with anti-mouse TNF-α or control IgG. Total RNA was extracted and expression levels of fibronectin and N-cadherin were measured using qRT–PCR. $*P<0.05$; CM, conditioned medium; Error bars, SDs; n.s., not significant.

to search for other secreted factors in the conditioned medium of RAW 264.7 cells that are able to enhance EMT of A549 cells. As shown in Fig. 6, the expression of IL-1β and IL-6, inflammatory cytokines produced by activated macrophages, was also detected in RAW 264.7 cells and upregulated by LPS (Fig. 6A). Similar to TNF-α, IL-1β significantly enhanced the expression of TGF-β-induced fibronectin and N-cadherin (Fig. 6B). In contrast, we did not observe such an effect following IL-6 treatment. Additionally, no cooperative effect of TNF-α and IL-1β was observed for TGF-β-induced expression of EMT markers (Fig. 6C). These results suggest that RAW 264.7 cells secrete multiple proinflammatory cytokines, including TNF-α and IL-1β, to enhance TGF-β-induced EMT in A549 cells.

Effect of NFκB inhibitor DHMEQ on EMT of A549 cells

We further attempted to evaluate the molecular mechanisms underlying enhanced TGF-β-induced EMT by TNF-α. A mixture of inflammatory cytokines has been reported to increase the expression of TGFBR1 encoding TβRI in A549 cells, leading to enhanced Smad2 phosphorylation (*35*). We also observed the upregulation of TGFBR1 mRNA by TNF-α, IL-1β and TGF-β (Supplementary Fig. 2A). However, phosphorylation of Smad2 did not change under our experimental conditions (Supplementary Fig. 2B). Furthermore, we found that TNF-α did not enhance the transcriptional activity of the 9xCAGA-luc reporter, which consists of tandemly repeating Smad binding elements (Fig. 7A), suggesting that TNF-α failed to activate TGF-β signals in the present experimental conditions. Activation of TNF-α-induced NF-κB signals was confirmed by the NF-κB-luc reporter, which was not activated by TGF-β. We also quantified the expression levels of several EMT-related transcriptional regulators by qRT–PCR. We found that expression levels of δEF1 and SIP1 were highest when the cells were stimulated with TNF-α, IL-1β and TGF-β (Supplementary Fig. 2C). In contrast, co-stimulation with TNF-α and IL-1β did not enhance TGF-β-induced expression of other transcriptional regulators. Therefore, δEF1 and SIP1 might function as downstream components of the TGF-β-induced EMT enhanced by TNF-α and IL-1β.

Finally, we studied the involvement of signalling pathways downstream of TNF-α and IL-1β in the enhancement of TGF-β-induced EMT. We examined the effect of the NFκB inhibitor DHMEQ on the enhancement of EMT by TNF-α and IL-1β. As a positive control, induction of the intercellular adhesion molecule 1 (ICAM-1) by TNF-α and IL-1β was efficiently inhibited by DHMEQ addition (Fig. 7B). Fibronectin expression was partially inhibited by DHMEQ, whereas that of N-cadherin was not affected (Fig. 7C). We also performed qRT–PCR analysis of A549 cells transfected with RelA small interfering RNA (siRNA). We observed that the expression levels of fibronectin in A549 cells transfected with three different siRNAs for RelA were lower than those in the cells transfected with control siRNA, which was in agreement with the result using DHMEQ (Supplementary Fig. 3). We then used several kinase inhibitors to examine whether other signalling pathways downstream of TNF-α and IL-1β enhance TGF-β-induced EMT. We found that U0126, an mitogen-activated extracellular signal regulated kinase kinase (MEK) inhibitor, weakly inhibited the induction of fibronectin expression (Fig. 8). We also found that SB203580, a p38 mitogen-activated protein kinase inhibitor, inhibited the enhancement of TGF-β-induced N-cadherin expression by TNF-α and IL-1β, though it upregulated the expression of N-cadherin, as well as that of fibronectin induced by TGF-β alone. Thus, NFκB, ERK and p38 pathways appear to play different roles as downstream components for both TNF-α and IL-1β.

Discussion

Previous studies focused on the roles of TGF-β and inflammatory cytokines on EMT during lung fibrosis and used A549 cells as a cell line of alveolar epithelial origin (*22*). Kasai *et al.* reported that TGF-β, but not TNF-α or IL-1β, induces EMT of A549 cells. Subsequent studies, however, revealed that TGF-β-induced EMT is augmented by either TNF-α or IL-1β (*36*, *37*), or a mixture of inflammatory cytokines which include TNF-α and IL-1β (*35*). Enhanced TGF-β-induced EMT by TNF-α was observed not only in A549 cells, but also in normal bronchial epithelial cells, suggesting that enhanced EMT by TNF-α may be important in other pathological processes of lung diseases (*21*, *38*, *39*). Recently, Borthwick *et al.* (*21*) reported enhanced TGF-β-induced EMT by co-culture of A549 cells with THP-1 human macrophage cells. However, they did not provide direct evidence that THP-1 cell-derived TNF-α is involved in the enhancement of TGF-β-induced EMT and did not study the molecular mechanisms involved. We utilized a neutralizing antibody against TNF-α, and revealed that endogenous TNF-α derived from RAW 264.7 cells plays an important role in the enhancement of TGF-β-induced EMT of A549 cells. We observed enhancement of TGF-β-induced EMT of A549 cells by stimulation of RAW 264.7 cells with LPS. It has been reported that LPS directly affects epithelial cells via its receptor TLR4. However, LPS neither activated NFκB pathway nor enhanced TGF-β-induced EMT of A549 cells in our analysis (Supplementary Figs. 1 and 4). Absence or reduced CD14 and TLR4 possibly explains such an impairment of LPS response of A549 cells in our condition (*40*, *41*). Partial inhibition of the effects of RAW 264.7-derived conditioned medium by the TNF-α antibody also suggested the importance of other secreted factors. Multiple inflammatory cytokines, including IL-1β, IL-8 and IL-6, are produced from activated macrophages. Whether endogenous IL-1β secreted from RAW 264.7 enhances TGF-β-induced EMT, should be evaluated in future studies. It has been reported that IL-8 does not exhibit this enhancing effect (*21*), and we did not observe enhancement of EMT by IL-6. We have not ruled out the possibility that enhanced EMT resulted from crosstalk between A549 cells and RAW 264.7 cells. The effects of cancer cells on macrophages have been extensively studied. For example, cancer cells produce the chemoattractant MCP-1. Versican, an extracellular matrix